sustainability

MDPI

Review

Overview of Model- and Non-Model-Based Online Battery Management Systems for Electric Vehicle Applications: A Comprehensive Review of Experimental and Simulation Studies

Neha Bhushan [1,*], Saad Mekhilef [1,2,*], Kok Soon Tey [3], Mohamed Shaaban [1], Mehdi Seyedmahmoudian [2] and Alex Stojcevski [2]

[1] Department of Electrical Engineering, Faculty of Engineering, Universiti Malaya, Kuala Lumpur 50603, Malaysia
[2] School of Science, Computing and Engineering Technologies, Swinburne University of Technology, Hawthorn, VIC 3122, Australia
[3] Faculty of Computer Science and Information Technology, Universiti Malaya, Kuala Lumpur 50603, Malaysia
* Correspondence: nehaphdmalaya@um.edu.my (N.B.); saad@um.edu.my (S.M.)

Abstract: The online battery management system (BMS) is very critical for the safe and reliable operation of electric vehicles (EVs) and renewable energy storage applications. The primary responsibility of BMS is data assembly, state monitoring, state management, state safety, charging control, thermal management, and information management. The algorithm and control development for smooth and cost-effective functioning of online BMS is challenging research. The complexity, stability, cost, robustness, computational cost, and accuracy of BMS for Li-ion batteries (LiBs) can be enhanced through the development of algorithms. The model-based and non-model-based data-driven methods are the most suitable for developing algorithms and control for online BMS than other methods present in the literatures. The performance analysis of algorithms under different current, thermal, and load conditions have been investigated. The objective of this review is to advance the experimental design and control for online BMS. The comprehensive overview of present techniques, core issues, technical challenges, emerging trends, and future research opportunities for next-generation BMS is covered in this paper with experimental and simulation analysis.

Keywords: lithium-ion battery; battery management system (BMS); electrical vehicle (EV); battery charging; battery modeling; states estimation and fault diagnosis

Citation: Bhushan, N.; Mekhilef, S.; Tey, K.S.; Shaaban, M.; Seyedmahmoudian, M.; Stojcevski, A. Overview of Model- and Non-Model-Based Online Battery Management Systems for Electric Vehicle Applications: A Comprehensive Review of Experimental and Simulation Studies. *Sustainability* **2022**, *14*, 15912. https://doi.org/10.3390/su142315912

Academic Editor: Talal Yusaf

Received: 30 June 2022
Accepted: 27 September 2022
Published: 29 November 2022

1. Introduction

Electric vehicles have become more prominent in cutting carbon emissions by at least 30–50%. LiBs are primarily used as an energy storage system for plug-in hybrid electric vehicles (PHEVs), hybrid electric vehicles (HEVs), and all-electric vehicles (EVs). The cost of a battery is a critical distinguishing factor between conventional vehicles and electric vehicles and needs to fall below 150 USD per kWh to make electric vehicles cost-effective [1]. LiBs have already captured 70% of the EV market (HEVs, PHEVs, and BEVs) due to their promising features such as great power, high energy density, light weight, fast charge capability, small self-discharge, and far-reaching life cycle compared to other batteries [2]. EVs experience high current rates, varying charge/discharge as they accelerate or brake, deep discharge conditions, low and high operating temperatures, and different working conditions [3]. Automotive battery management systems (BMSs) require estimating the remaining energy for range calculation, limiting power for acceleration, regenerative braking for cost-effectiveness, and calculating cycle life for safety. It is challenging as the vehicle works in real time with changing road conditions, driving styles, temperature, and electromagnetic interference, which can make the battery system complex, time-varying, and nonlinear [4,5]. The essential features of the BMS comprise data collection, state monitoring, cell balancing, thermal management, safety, charging control, and information management. The challenges associated with online BMS systems are given below.

(1) The challenge for the state-of-charge (SOC) estimation is the great amount of current in EVs, leading to complex dynamics that are difficult to capture using a battery model.
(2) It is very difficult to predict battery aging or state of health (SOH) online by measuring current, voltage, and temperature. No sensor has been developed yet to predict online capacity and internal resistance.
(3) The battery state of power (SOP) and state of energy (SOE) also depend on aging (SOH) and SOC. Therefore open-loop experimental methods such as ampere-hour counting (AHC), and open-circuit voltage (OCV) are not suitable for online state monitoring of BMS. The development of an algorithm to work on the relationship of battery state with the combined estimation of all these measurements is challenging for online BMS.
(4) The state of safety (SOS) depends on multi-fault diagnosis, which is still challenging to achieve online.
(5) Fast and optimized charging is crucial for EVs. It is challenging to optimize charging methods to prolong cycle life and enhance safety, speed up charging time, and increase charging performance.

A comprehensive literature review was carried out on BMSs, including Li-ion charging techniques, battery modeling, states estimation, cell balancing, and fault diagnosis [6–14]. This paper's contribution is to develop the idea for an online BMS, which is essential for the safety, cost, and reliable operation of an automotive vehicle. The algorithm development of model-based and non-model-based (data-driven methods) is best for online BMSs. A comprehensive review with experimental and simulation studies for online BMSs in electric vehicle applications is performed from a technical perspective in the present paper. The main objectives of this paper are as follows:

(1) Model-based and non-model-based (data-driven methods) algorithm development for online state monitoring for complex, nonlinear, and time-varying battery systems. SOC, SOE, SOH, and SOP estimation is the prime objective of the BMS.
(2) Algorithm development for battery state of safety (SOS), control, and fault diagnosis, which is essential for BMS condition monitoring.
(3) Algorithm development for charging control, which is crucial as the charging process of the LiBs directly impacts the SOH and SOS of LIBs. Model- and non-model-based charging optimization strategies are key to the safety and longevity of LiBs.

Each section of the present paper provides an in-depth observation, analysis, issues, challenges, and future directions. Section 2 presents charging algorithms for enhancing battery life and safety. In Section 3, the electrochemical model (ECM), analytical model (AM), equivalent circuit model (ECM), thermal model (TM), electro-thermal model, hysteresis model, fractional-order model, and integer-order model are discussed [15–17]. Section 4 presents the algorithm development for online parameter and state estimation. The model-based algorithm development for online state estimation of LiBs is discussed in depth. The Kalman filter algorithm and its variants are discussed for model-based online parameter and state estimations in Section 5. In Section 6, data-driven-based online battery state monitoring is presented [18]. The unique contribution of this section is to develop emerging deep learning algorithms for online state forecasting for EVs. Section 7 explores algorithm development for model- and non-model-based fault diagnosis and control for BMSs. Section 8 concludes this review. These elements were unexplored in past literature reviews.

The Panasonic NCR18650B, A123 LFP 26650, Sony Murata 18650 VTC6, and A123 LFP 18650 cells were chosen for battery testing at different temperatures. The BTS-4000 battery cycler and temperature chamber were used for testing. Simulations were performed with MATLAB 2020, Jupyter notebook, and python framework.

2. Lithium-Ion Charging Strategy for Electric Vehicles

The charging time, loss, and control are significant concerns in BMS for E.V. applications. The charging and discharging of Li-ion batteries are very important for obtaining battery characteristics [19]. The various vital factors on a cell level, module level, and system level affect the performance of the vehicle's charging level. The optimal charging profile to control charging loss, charging time, battery aging, and balance with charging speed, charging polarization, and temperature rise is challenging research in this area. The various charging algorithms proposed in the literature that are most popular are CC-CV, CP-CV, MCC-CV, VCP, boost, and pulse charging. The current-controlled and voltage-controlled charging methods are very popular for charging the battery with constant current and voltage. If we apply a small current, then efficiency is increased, and battery temperature and voltage do not increase sharply. A higher current takes less time to charge, but efficiency is compromised, and the temperature and the voltage can rise. Overvoltage can avoid the constant voltage method but a very high current, in the beginning, causes a reduction in battery life. Therefore, a hybrid approach came into existence called CC–CV (constant current–constant voltage), which integrates the two control methods to improve charging efficiency, battery life, and safety [6,20].

The model- and non-model-based optical charging profile has been discussed in various studies. In [21], the moth-flame optimization (MFO) algorithm was used to propose a fractional model-based multistage charging strategy that divides the charging current into various phases. The charging time, temperature rise, and energy loss are chosen as optimization goals in consideration of the safety and efficiency of the charging procedure. The MFO algorithm, which benefits from a straightforward structure and great local search capability, is used to enhance charging performance. In [22], the fast-charging Bayesian optimization approach suggested explicitly contained limitations that prevent degradation. The suggested BO-based charging methods do not need first-principles models and are sample-efficient. Different charging algorithms and key features are described in Table 1.

Table 1. Key features of charging algorithms.

Charging Algorithm	Characteristics of Algorithm	Variants of the Charging Algorithm	Comparison
Simple charging method	This charging protocol includes controlled constant current and voltage to avoid a sharp increase in the battery's temperature and voltage. Trickle charging is a low-current charging method when the battery is in a deep discharge state. It shifts to CC mode until voltage reaches a threshold value.	Constant current charging (CC) Trickle charging Standard CC charging Constant voltage charging (CV)	Simple, cost-effective, but not currently popular compared to other charging protocols.
Constant current–constant voltage (CC–CV) [23]	CC is applied to charge the battery until the predefined voltage level after switching to the CV mode until the charge current reaches a minimum threshold.	Double-loop control charger (DL-CC/CV) [24] Boost charger (BC-CC/CV) [25] Fuzzy logic (FL-CC/CV) [26] Gray-predicted (GP-CC/CV) Phased locked loop (PLL-CC/CV)	Most popular, simple, and inexpensive regarding other charging protocols.

Table 1. *Cont.*

Charging Algorithm	Characteristics of Algorithm	Variants of the Charging Algorithm	Comparison
Duty-varied voltage pulse charger (DVVPC) [27]	The duty-varied voltage pulse charger can notice the appropriate pulse-charge duty and supply the battery's required pulse charge.	DFVPCS (duty-fixed voltage pulse charger)	The charging speed is improved compared to CC–CV.
Multistage constant current (MSCC) [24,28,29]	This protocol comprises variable current magnitude with two or more constant current stages where shifting conditions are based on upper cutoff voltage or SOC interval.	Optimal five-stage charging protocol using consecutive orthogonal arrays [25]. Optimal multistage charging pattern using PSO-based fuzzy controlled [26]. Optimal charging pattern for MSCC [28]. MSCC charging pattern is based on the integration of the Taguchi method and SOC estimation [30]. The ant colony algorithm is been used for implementing the MSCC-based optimal charging method [31].	MSSC protocol can decrease the charging time and enhance the charging efficiency. Lower charging time and capacity fade compared to CC–CV.
Boost charging [32]	This protocol is used for fast charging in which a fully discharged cell is charged with a very high current for a short period without degradation.	CVCCCV	It is a rapid charging protocol that can charge one-third of battery-rated capacity in 5 min compared to other protocols [32].
Pulse charging [33,34]	Noncontinuous CC and CV can be defined as pulse charging.	Constant current + pulse charging (CCPC) [33] Constant-current and constant-frequency pulse charging (CCCF-PC) Constant-current and variable-frequency pulse charging (CCVF-PC) Variable-current and constant-frequency pulse charging (VCCF-PC) Variable-frequency variable-current pulse charging Pulse charge with constant voltage (CVPC) [27]	Cost-effective and straightforward with respect to other charging schemes.

Table 1. *Cont.*

Charging Algorithm	Characteristics of Algorithm	Variants of the Charging Algorithm	Comparison
Variable current profile [35]	Noncontinuous CC and CV can be defined as pulse charging.	Constant current + pulse charging (CCPC) [33] Constant-current and constant-frequency pulse charging (CCCF-PC) Constant-current and variable-frequency pulse charging (CCVF-PC) Variable-current and constant-frequency pulse charging (VCCF-PC) Variable-frequency variable-current pulse charging Pulse charge with constant voltage (CVPC) [27]	Slower aging effect compared to CC–CV [36].
Sinusoidal ripple current [37]	This charging protocol superimposes the low-frequency sinusoidal current on a DC current.	SRC + CP SRC + CT	The cycle life, temperature rising, charging time, and charging efficiency are better than CC–CV [37].
Constant current–constant voltage with negative pulse (CC–CV-NP) [38,39]	This charging protocol improves the low-frequency sinusoidal current at the time of CC to delay the polarization that enhances the battery charging capacity and slows down the aging.	MCC–CVNP	CC–CVNP charging protocol with small amplitude and a minimum number of negative pulses is more efficient than other protocols in lowering the diffusion time constant and concentration polarization resistance. This property increases the charging efficiency and longevity [38].
Constant-power–constant-voltage (CP–CV) [24,40]	In the CP–CV charging protocol, the current starts at a high rate and steadily decreases with the charging time. In the meantime, a CP co-relation exists between the current and voltage. CV charging is followed by voltage reached to its maximum cutoff until the current decreases to a predefined value.	CP	At a low charging rate, capacity fade is in the order of CP > MCC > CC. At a high charging rate, capacity fade is in order of MCC > CC > CP [24].
Constant temperature–constant voltage (CT–CV) [41,42]	The optimal CT–CV charging protocol controls the charging current magnitude corresponding to the temperature of the cell. It is a closed-loop technique that modulates the charging current concerning the battery's temperature.	CT + SRC CT + PC	CT–CV is a fast-charging and low-temperature rise method compared to CC–CV.

2.1. Simulation Comparison between CC–CV and CP–CV Charging Profile for EVs

As shown in Figure 1, SOC increases over time linearly in the constant-current portion during a test, while SOC still increases but not as quickly after switching to the constant-voltage portion. Therefore, the graph's slope possesses a nonconstant value as SOC steadily proceeds to desired final values. The above result is also manifested as one reason that the system charges rapidly until 80–90%, before taking a long time to reach 100% SOC or exceeding the manufacture voltage of the cell. The first interval current remains constant in the graph, demonstrating the relationship between power and time. However, the magnitude of power increases with an increase in voltage. The magnitude of power increases with an increase in voltage. In the second interval, the current magnitude continuously decreases; hence, the power magnitude decreases over time. The sign value increases, but the magnitude decreases.

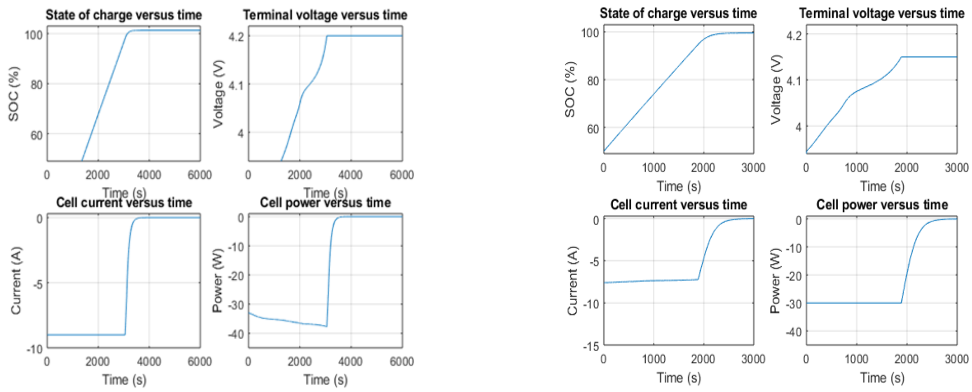

(**a**) (**b**)

Figure 1. Simulation results charging a cell from 50% SOC to maximum voltage with (**a**) CC/CV and (**b**) CP/CV. Adopted from [43].

2.2. Issues, Challenges, and Future Directions

Several charging algorithms and controls were discussed in the present paper, but there is room for improvement in this area, as discussed below.

(1) The waveform-based charging techniques include CC–CV, SCV, and the pulse charging usage open-loop technique based on previous information on cell parameters. MSCC charging protocols implement optimization algorithms to overcome this limitation. Sometimes these optimized algorithms also take numerous charge/discharge cycles to converge at the expected profile. There is also the possibility of temperature and parameter variation before the optimization algorithm resolves. There is a requirement for optimization algorithms that can close the loop in shorter time frames using cell parameters/temperatures to regulate the charging current magnitude.

(2) The scope of improving the smooth optimal charging current profile is to reduce noise in temperature, current, and voltage sensors.

(3) experimental optimization should be adopted to save time and cost of BMSs. Machine Learning can be utilized for closed-loop optimization of charging protocols for LiBs.

3. Li-Ion Battery Modeling

There are different types of modeling techniques defined in the literature for EV application, in which electrochemical models (ECM), analytical models (AM), data-driven models (DD), electrical equivalent circuit models (EECM) or equivalent circuit (EC) models, thermal models (TM), and electro-thermal models are usually discussed (Figure 2).

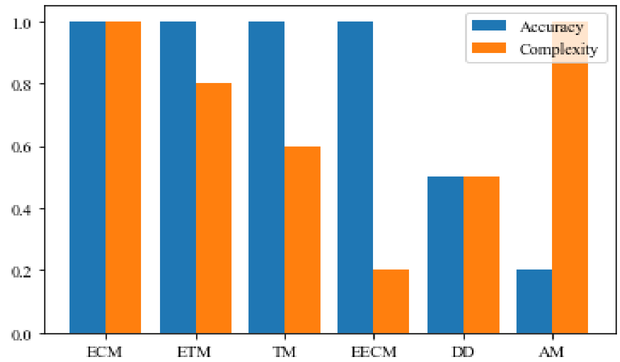

Figure 2. Accuracy and complexity comparison of different modeling techniques.

Electrochemical models (ECMs) develop the scientific understanding to enhance and optimize the physical design (electrodes and electrolyte) features of Li-ion cells, describe the power generation tools, and perform a multiscale approach to understand the macroscopic (battery voltage and current, discharge/charge, capacity, power, and SOC) and microscopic (SOH, aging, and durability) physiochemistry [44,45]. Electrochemical modeling is not accessible for dynamic and system-level modeling as they include the system of coupled time-variant nonlinear partial differential equations with a significant number of unknown parameters, which is time-consuming, complex, and computationally and resource-intensive as battery-specific information is also needed [46]. Simple circuit-based models (EC) are suitable for vehicle applications [47,48]. The modeling is the electrical representation of battery behavior under different driving profiles or loads. EC represents the terminal voltage reaction under distinct load types or driving profiles for dynamic and nondynamic (resistive) methods. The RC circuit defines the battery's dynamics. The equivalent circuit model simulates the dynamic characteristics and estimates SOC, SOH, available power, and energy using resistance, capacitance, a voltage source, and another circuit component to form a circuit.

The Li-ion battery's performance under varying drive cycle conditions depends on the different operating temperatures and charge/discharge rates. Battery performance highly depends on thermal conditions such as low temperature, high temperature, thermal runaway, abuse based on overcharging, over-discharging, high C-rates, and external heating. The key objective of thermal modeling (TM) and electro-thermal modeling (ETM) is to avoid exceeding the heat dissipation rate to avoid the thermal runaway of a cell. Determining the effect of battery parameters on temperature dynamics is also a reason for thermal modeling. We need to model the heat generation rate and dissipation in a cell to perform actual thermal management in battery packs. There are multiple types of thermal models for original applications available in the literature, such as experimental, lumped parameter, multiscale, multidimensional, and multi-physics models including thermal–electrochemical coupled, SPM, pseudo, 2D, and 3D models. Zhuo Yang [49] proposed the electrical and thermal behavior of the cell under different drive cycles. These electrothermal model parameters are dependent on temperature and current rate. Tedjani et al. [50] proposed a dynamic battery model focused on voltage, temperature, and the aging phenomenon and offered the dynamic relationship among battery electric, thermal, and aging behavior to test the exactness of range. Tarun Huria proposed a high-fidelity electric model with the thermal dependence of Li-ion batteries for characterization and simulation [51]. This model can express nonlinear electrochemical phenomena and is suitable for system-level modeling (ex-power-train electrification).

3.1. Electrical Equivalent Circuit Model (EECM) or Equivalent Circuit Model (ECM) of Li-Ion Batteries

The EECM modeling of Li-ion cells or packs is system-level modeling mainly developed for applications such as EVs. The battery modeling is crucial in estimating battery parameters, including OCV, internal resistance, RC networks, terminal voltage, polarization voltage, and states, including SOC, SOE, SOH, SOP, SOF, and SOS [52,53]. The equivalent circuit model (ECM) is a tradeoff between complexity and accuracy. ECM is easily well-suited to the circuits of BMSs and easily embedded into BMSs for EVs. Table 2 presents the battery models used extensively in the literature. The accuracy of the ECM mainly depends on its states, parameter, current rate, temperature, and environmental or operating conditions. It also reflects the nonlinearity and hysteresis effect under a high and dynamic current rate for EVs [54].

Table 2. Comparison of battery models and discretization equation for EV applications [55,56].

Models	Equation and Description	Parameters/Optimization	Applications
1RC	$V_k = OCV(soc_k) - I_k R_0 + u_{1,k}$ $u_{1,k} = \exp(-\Delta t/\tau_1)u_{1,k-1}$ $+ R_1[1 - exp(-\Delta t/\tau_1)]I_k$ $V_k = terminal\ voltage$ OCV = open circuit voltage, soc_k = state of charge, R_0 = internal resistance, $I_k = current$ $u_{1,k}$ = voltage of RC network, $\tau_1 = R_1C_1$ = time constant of RC network	4/FMIN	This model is the perfect selection for NMC chemistry.
1RCH	$V_k = OCV(soc_k) - I_k R_0 + u_{1,k} + u_{h,k}$ $u_{h,k}$ = voltage of hysteresis network	FMIN	1RCH-based online SOC, SOH estimation, which is applicable in EVs and PHEVs. Further enhancement can be achieved with SOP and SOF analysis. Thermal and aging effects can also be integrated with this model. This model is the best fit for LFP cells.
2RC	$V_k = OCV(soc_k) + I_k R_0 + u_{1,k} + u_{2,k}$ $u_{2,k} = \exp(-\Delta t/\tau_2)u_{2,k-1}$ $+ R_2[1 - exp(-\Delta t/\tau_2)]I_k$ $u_{2,k}$ = voltage of 2RC network, $\tau_2 = R_2C_2$ = time constant of 2RC	6/PSO	The 2RC model demonstrates a balance between accuracy and complexity, making it the preferred choice for EV applications.
2RCH	$V_k = OCV(soc_k) + I_k R_0 + u_{2,k} + u_{h,k}$	8/PSO	The 2RCH model does not advance its accuracy but reduces its reliability in the case of parameter estimation; thus, it is not a correct choice for EV application.
3RC	$V_k = OCV(soc_k) + I_k R_0 + u_{1,k} + u_{2,k} + u_{3,k}$ $u_{3,k} = \exp(-\Delta t/\tau_3)u_{3,k-1}$ $+ R_3[1 - exp(-\Delta t/\tau_3)]I_k$ $u_{3,k}$ = voltage of 3RC network, $\tau_3 = R_3C_3$ = time constant of 3RC	8/FA	Not appropriate for online identification of parameters and states
3RCH	$V_k = OCV(soc_k) + I_k R_0$ $+ u_{1,k} + u_{2,k} + u_{3,k} + u_{h,k}$	10/FA	Not appropriate for online identification of parameters and states.
4RC	$V_k = OCV(soc_k) + I_k R_0$ $+ u_{1,k} + u_{2,k} + u_{3,k} + u_{4,k}$ $u_{4,k} = exp(-\Delta t/\tau_4)u_{4,k-1}$ $+ R_4[1 - exp(-\Delta t/\tau_4)]I_k$ $u_{4,k}$ = voltage of 4RC network, $\tau_4 = R_4C_4$ = time constant of 4RC	10/FA	Not suitable for online BMS applications for EVs.
4RCH	$V_k = OCV(soc_k) + I_k R_0$ $+ u_{1,k} + u_{2,k} + u_{3,k} + \mu_{4,k} + u_{h,k}$	12/FA	Not suitable for online BMS applications for EVs.

In Table 2, the comparison of battery models is discussed with suitability for EV applications. A more significant number of RC networks can yield all three characteristics (ohmic resistance, diffusion voltage, and charge transfer). However, the complexity and computation burden also increase with an increasing number of parameters. More RC networks can produce the problem of overfitting and raise the exertions for system standardization.

3.2. Fractional-Order Battery Model

Fractional calculus was introduced for Li-ion applications to address the problem of identifying ohmic resistance, charge transfer, and diffusion characteristics [57]. An infinite-dimensional model was established by interchanging the ideal capacitor in the 1RC model with a constituent element. The Oustaloup recursive approximation in which lower- and upper-frequency limits impact poles and zeros of the model's transfer function has been approved to simplify numerical calculations that affect model accuracy. This type of model can replicate Li-ion battery characteristics better than the integer model by using data from the time and frequency domain with fractional order (additional degree of freedom) [58,59]. The fractional-order model (FOM), with a constant phase element (CPE), is the same as the integrated order model with a 5RC element. Adding the Warburg element in series with a charge-transfer resistor leads to accomplishing greater accuracy of the FOM [57,59]. In [60], an SOC estimation approach for lithium-ion batteries based on a temperature-based fractional first-order RC circuit model and dual fractional-order Kalman filter (DFOKF) was presented in order to investigate the temperature requirement of battery modeling and SOC estimation. In [61], to improve the accuracy of the battery SOC estimation, a multiscale fractional-order dual unscented Kalman filter was suggested. It was proposed to use a fractional-order model (FOM) based on the theory of fractional calculus to represent the properties of lithium-ion batteries. The adaptive genetic algorithm was used to identify its parameters, see Figure 3.

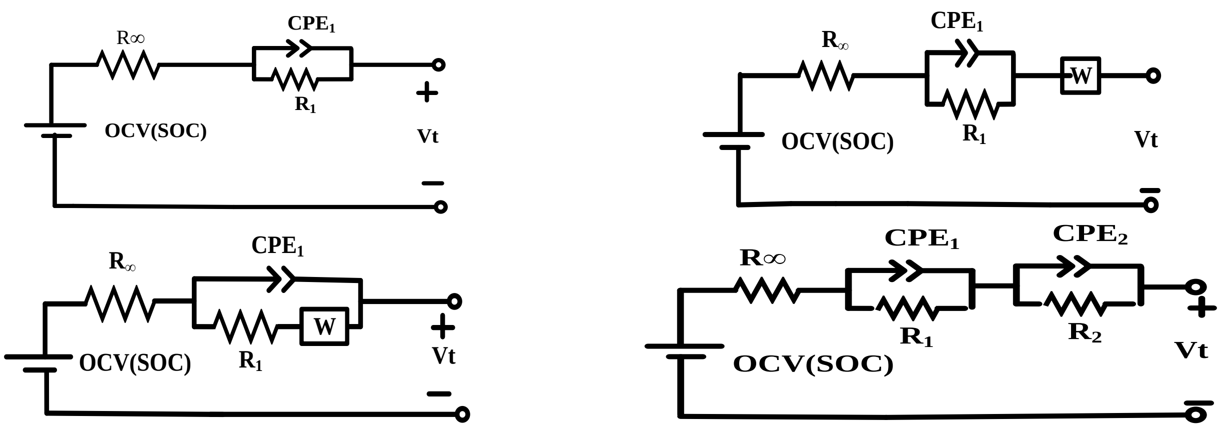

Figure 3. Example of a fractional-order model of Li-ion cell [62].

3.3. Issues, Challenges, and Future Directions

1. An excellent battery model should predict battery dynamics in both time and frequency areas in complete operating conditions. The ideal model for BMS should be performed with modest parameter identification, less computation burden, and good accuracy in different operating conditions. The existing model needs to be modified with a better algorithm to make parameter and state identification secure and robust.
2. The main disadvantage of FOM is a computationally expansive procedure for employment in BMS, and an intelligent management algorithm is technically very challenging. Future research in this direction needs to be carried out.

4. Model-Based Online Parameter and State Estimation

Algorithm development for online state and parameter estimation is quite challenging in terms of cost, complexity, accuracy, noise immunity, tuning effort, and convergence property due to nonlinear dynamic behavior. The parameters of the battery include OCV, impedance parameters (ohmic resistance and polarization resistance), capacity parameters, time constant, and voltage polarization, which are slow-varying. On the other hand, battery states such as SOC, SOP, SOE, and SOF are fast-varying, SOT is intermediate varying, SOH is slow-varying, and SOS has adjustable fast-level states [63]. Estimation of each parameter and state at a similar timescale increases the cost and complexity of BMS. The frequent update of parameters would make the parameters fluctuate acutely and impact the estimation of the battery's state [64]. The key issues in online estimation of states are discussed in Table 3.

Table 3. Key issues in online state estimation.

States	Equations	Challenges in Automotive Applications	Methods
State of charge (SOC) [65]	$SOC_{K+1} = SOC_k - \left(\frac{\eta_i \cdot T_s}{Q_n}\right) i_k$	The main challenge of SOC estimation in automotive applications is the great amount of current produced in these types of applications, leading to stimulating complex dynamics that are difficult to capture using EECM.	1. Direct calculation method 2. Coulomb-counting methods 3. OCV–SOC relationship 4. Model-based method 5. Data-driven method
State of health (SOH) [66]	$\eta_i = \frac{Q_{discharge}(Ah)}{Q_{charge}(Ah)} \times 100\%$	The major challenge related to the online estimation of SOH by measuring current, voltage, and temperature measurement is the complexity, which means it is very hard to predict the battery aging growth. Currently, no sensor is available to directly measure capacity and internal resistance.	1. Experimental method 2. Model-based estimation 3. Incremental capacity analysis (ICA) and differential voltage analysis (DVA) method 4. Empirical models 5. Data-driven method 6. Waveform-based method.
State of power (SOP) [7]	$P_{dis,k} = \frac{V_{\min}\left(V_{OC,k} - V_{\min}\right)}{\hat{R}_{eq}}$, $P_{ch,k} = \frac{V_{\max}\left(V_{\min} - V_{OC,k}\right)}{\hat{R}_{eq}}$	The SOP prediction depends on current, voltage, temperature, and SOC, and these parameters are still not optimized. The SOP also depends on battery aging, which is difficult to predict online.	1. Characteristic map (CM)-based method 2. Model-based method 3. Multiple constant estimation approach 4. Data-driven approach
State of function (SOF) [53]	$SOF = \begin{cases} 1, & \text{for } P_{ch,k} \geq P_{req}^{ch} \text{ and } P_{dis,k} \geq P_{req}^{dis} \\ 0 & \text{for } P_{ch,k} < P_{req}^{ch} \text{ and } P_{dis,k} < P_{req}^{dis} \end{cases}$	The main challenge in SOF estimation is the deficiency of an accurate model to relate SOC, SOH, SOF, and temperature.	1. Model-based method 2. Data-driven approach
State of energy (SOE) [67,68]	$SOE(t) = SOE(t_0) + \frac{\int_{t_0}^{t} P(\tau) d\tau}{E_N}$	The power integration is used for estimating SOE, which enhances the computational complexity. In another way, its open-loop nature results in accumulated errors leading to measurement flaws, uncertain noise, and restricted sensor resolution.	1. Direct estimate 2. Power integration approach 3. Characteristic mapping approach 4. Adaptive algorithm estimation 5. Machine learning method
State of temperature (SOT) [69]	$C_c \frac{dT_c}{dt} = \dot{Q} + \frac{T_s - T_c}{R_c}$ $C_s \frac{dT_s}{dt} = \frac{T_{amp} - T_s}{R_u} - \frac{T_s - T_c}{R_c}$ $\dot{Q} = I(U - V) + I(T \frac{\partial U}{\partial T})$	Online estimation is quite difficult due to computational efficiency.	1. Impedance–temperature detection (ITD)-based method 2. Model-based method 3. Integrated method
State of safety (SOS) [70]	$H_r = H_s \cdot H_l$	Practical online estimation is not possible for SOS. The fidelity of SOS is not guaranteed.	1. Qualitative estimation 2. Quantitative estimation

4.1. Model-Based Online Parameter and State Estimation of Li-Ion Battery

The model-based online state estimation is classified as experimental techniques that include direct measurement (AHC and OCV) and an adaptive approach (filters, observers, etc.). The model-based estimation is the most popular and robust method for SOC and SOH estimation because of the continuous error-correction tool via closed-loop feedback. In Figure 4 and Table 4, important adaptive approaches are presented for model-based state estimation. A popular method for identifying unknown parameters for linear ECM is the least square method, which lessens the sum of squared residuals. The least-square filters include recursive least square (RLS) and weight recursive least square (WRLS), as well as non-recursive least square, which also supports iterative LS but is cost-effective in terms of memory saving and computation [71,72]. The Luenberger observer is a simple algorithm to determine a feedback gain which modifies SOC by comparing the model voltage and measured voltage [73]. In [74], battery state-of-health monitoring and remaining usable life (RUL) prediction were investigated using an enhanced particle filter (PF) technology. In [75], to achieve a precise SoC estimate, a terminal sliding mode observer (TSMO) algorithm based on a hysteresis resistor–capacitor (RC) equivalent circuit model was implemented. The federal urban driving schedule (FUDS) test and the dynamic street test (DST) are two dynamic battery tests used to assess the proposed approach. The outcomes of the simulation demonstrate that the suggested strategy produced excellent estimation accuracy and fast convergence. Changes in temperature and loading current have a direct impact on how well SOC is estimated. The adaptive H-infinity filter (AHIF) can fully accommodate the fractional-order model and operation condition differences created by various temperatures and loading currents based on reliable parameter identification [75]. The Kalman filter and its variants have been used frequently and successfully for the estimation of various states due to their superiority compared to other algorithms. The next section is focused on the Kalman filter and its variants for different state estimations.

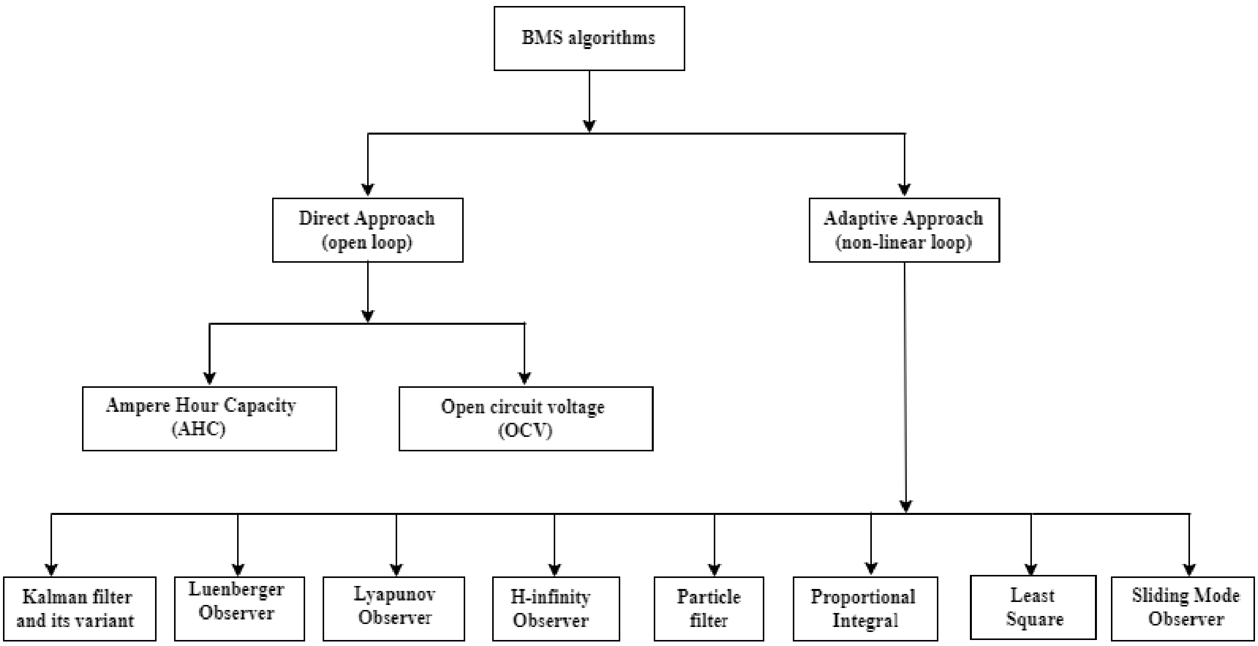

Figure 4. Algorithm development for model-based online parameter and state estimation.

Table 4. Algorithms development of model-based online parameters and states estimation.

	Methods	Strongpoint	Drawback or Error-Source	Applications	Predicted Error
Direct approach (open loop)	AHC [76,77]	AHC requires the information of current battery capacity It is a simple current-based estimation method (charging/discharging) and integrated over time Low-power computation Cheap sensor for current measurement Can be combined with other techniques	Open-loop and uncertain initial SOC (cumulative effect) Sensitive to the current sensor	AHC collaboration with adaptive algorithms is a satisfactory choice for HEVs	Enhanced AHC method for SOC and SOH estimation and estimation error reduced to 1.08% SOC estimation error under 6.5% using online EKF-AH
	OCV [73,78]	Secure and capable method for BEVs and HEVs Relationship between OCV-SOH determined by observing charging curves at the altered lifespan of Li-ion battery to predict model parameters and capacity fade to evaluate SOH [57] Simple and easy to implement, look-up table-based method	Not suitable for battery chemistry having flat OCV–SOC curves Open loop Quickly responds to the voltage-sensor precision	AHC corrected by OCV and state estimation is a satisfactory choice for BEVs and PHEVs	Integration of (AHC + OCV + KF) precisely estimates SOC compared with the OCV estimation method with an error of $\pm1.76\%$
Adaptive approach (nonlinear, -loop)	KF and its variants [79–81]	The KF requires models and measurement noise These algorithms help reduce measurement noise effects and predict the states (SOC and SOH) that cannot be estimated straightforwardly It is closed-loop, accurate, and error-bounds	The KF is dependent upon model accuracy It is a highly complex and expansive computation Several variables need to be controlled	All types of EVs	DEKF ($\pm5\%$) AEKF (MAE (0.02)) DEKF ((±0.01)
	Luenberger observer [82,83]	Faster than KF and suitable for all chemistry Does not depend on model and measurement noise Neither noise is Gaussian	These observers have high computational complexity They require a robust controller. PF acquires high computational complexity (approximately thousandfold) in comparison with EKF/SPKF	All types of EVs	1.25%
	Lyapunov observer [84]	Better accuracy, convergence time, robustness, chattering, and computational complexity			0.59%
	H-infinity [85,86] Observer	These observers can enhance the feature of the feedback gain, leading to accurate SOC estimation.			1%
	Sliding-mode observer [87,88]	Upgrade tracking control for stability and robustness			$\leq\pm3\%$
	Particle filter (PF) [89,90]	Robust and low computation time			$\leq1\%$
	Proportional integral (PI) [91]	More robust with model uncertainty			$\leq2\%$
	Least square [92–94]	Takes less execution time and lower algorithm complexity			0.05

4.2. Issues, Challenges, and Future Directions

(1) For more accurate and reliable model-based state estimation (SOC/SOH/SOP/SOF), multi-model fusion technology has been newly proposed (Figure 5) to increase model adaptation with a different operating condition, environment, and cycle life.

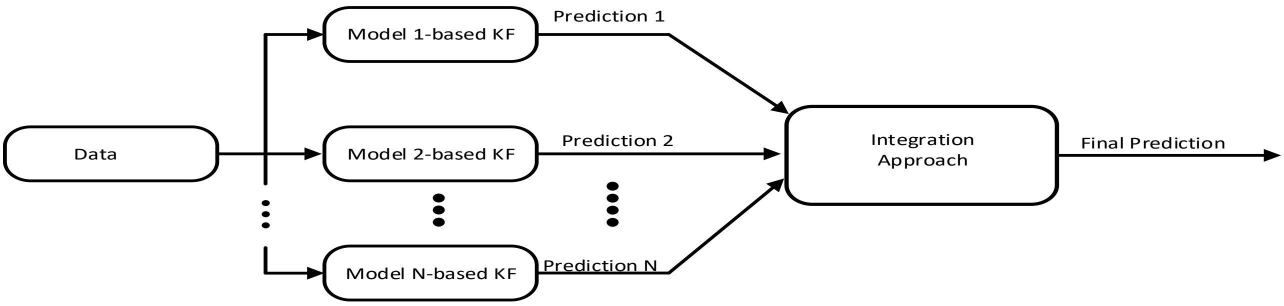

Figure 5. Multi-model fusion technology [95].

(2) To decrease the complexity and computational cost, multi-timescale, dual, joint, and combined state and parameter estimation should be adopted.

5. Kalman Filter Algorithms for Model-Based Online Parameter and State Estimations

The most popular and precise, but expensive parameter estimation method is the Kalman filter family (KF) of algorithms, which are recursive procedures to calculate applicable feedback gain. KF is only applicable for linear models, leading to the development of the extended Kalman filter (EKF) for nonlinear models to determine optimal filter gain and noise, which still lacks robustness and is not the right choice for optimal feedback gain due to the linearization of nonlinear LiBs [16]. Further improvement in this family includes the sigma point Kalman filter (SPKF), central difference Kalman filter (CDKF), and unscented Kalman filter (UKF), which are more robust and have better feedback but have increased computation complexity due to mandatory matrix inversion that enhances numerical instability primarily in the case of higher-dimensional model matrices [96–98]. The fractional-order KF also needs to be applied to a special battery model that includes fractional-order elements [66].

Table 5 compares the Kalman filter and its variants for state estimation on the basis of an extensive literature review.

Table 5. Comparison according to tradeoff between complexity, execution time, and cost.

A Variant of the Kalman Filter	Estimation Accuracy	Estimation Error MAE (%)	Convergence Speed	Complexity	State Estimation	Computational Cost
EKF [99]	Strong robustness against current noise	0.01	UKF convergence rate is better in the case of unknown initial SOC	Medium	SOC	Medium
UKF [98]	Superior to EKF in terms of robustness	0.63	Less than EKF due to state vector sigma point (2n + 1).	The implementation is not simpler due to more tuning parameters, but filter robustness is high.	SOC	4 times higher than EKF
AEKF [95]	Better accuracy and higher robustness than EKF	0.54	Improved due to outstanding OCV–SOC relationship	High	OCV and SOC	High
AUKF [76]	Better than UKF and AEKF	0.038	Better than UKF and AEKF	High	RUL	High
CDKF [77]	Better in estimation accuracy, filter robustness, and implementation	0.0096	More than EKF	It is simpler in implementation than UKF due to only one tuning parameter	SOC	High
SR-CDKF [78]	Better accuracy than EKF, UKF, and CDKF Robust to current noise	2%	Less than EKF and UKF	Non-negative covariance and reduced computational complexity	SOC	High

Table 5. *Cont.*

A Variant of the Kalman Filter	Estimation Accuracy	Estimation Error MAE (%)	Convergence Speed	Complexity	State Estimation	Computational Cost
SR-UKF [77]	Strongly nonlinear and more accurate than EKF, UKF, and CDKF	0.0022	More than EKF, UKF, and CDKF	High	SOC	High
Asymmetric ASR-SPKF [96]	More accurate than AEKF	2	Faster convergence speed	Less complex than AEKF and ASPKF	SOC	Less than ASPKF
SP-UKF	Like true value	1	Moderate convergence speed	More complex than SP-UKF	SOC, SOH, SOP, and SOE	Computationally intensive
SP-CDKF	Superior performance to EKF and SP-UKF	1	Faster convergence speed	Only one control parameter rather than three control parameters of SP-UKF	SOC and SOE	Computationally intensive
ACKF [79]	Good robustness	4	Good convergence capacity	Better than CKF	SOC	Better than CKF
CKF [100]	More robust than EKF and UKF	1	Faster than UKF but slower than EKF	CKF with the Thevenin model is a better option for embedding in microcontrollers	SOC	4 times higher than EKF
ST-CKF [80]	Robust	1.8	Moderate convergence speed	High	SOC	High
SR-CKF [81]	Higher accuracy and robustness than EKF, UKF, and CKF	0.00015	Higher convergence rate than EKF, UKF, and CKF	Less	SOC	More than EKF, UKF, and CKF
BS (backward smoothing)-SRCKF [82]	Improved accuracy	0.55	Improved convergence speed, faster than UKF and SRCKF	High than SRCKF but less than UKF	SOC, SOH, and RUL	High
QKF, Szego quadrature (SQKF) [83]	High accuracy, overcome the impact of large measurement and initial error	0.892	Convergence to 4% in 672 steps	High	SOC	High
Square-root transformed cubature quadrature Kalman filter (SR-TCQKF) [84]	More stable and accurate than CQKF	1	Improved convergence speed due to square root KF	Less, better numerical stability	SOC	Less

5.1. Algorithm Comparison of Simulation Results of EKF and SPKF

Ref. [101] demonstrated the implementation of EKF on the ESC model (Figure 6a,b; simulation data adopted from [101]). The author performed a test where EKF was executed for dynamic profiles (UDDS drive cycles separated by rest intervals) from 100% SOC to 3.3% SOC. The RMS error calculated for SOC estimation in the second figure was 1.53%, whereas the time error outside bounds was 35.9%. The test achieved 50 C with nonlinear hysteresis in cell voltage. A better estimation was possible with an increase in temperature. The SPKF was implemented using the same model and data, and the estimation RMS error was 0.84% (Figure 7a,b). The estimation error was within the bound of the SPKF filter 10.5% of the time. This result of SPKF with compared to EKF is remarkable.

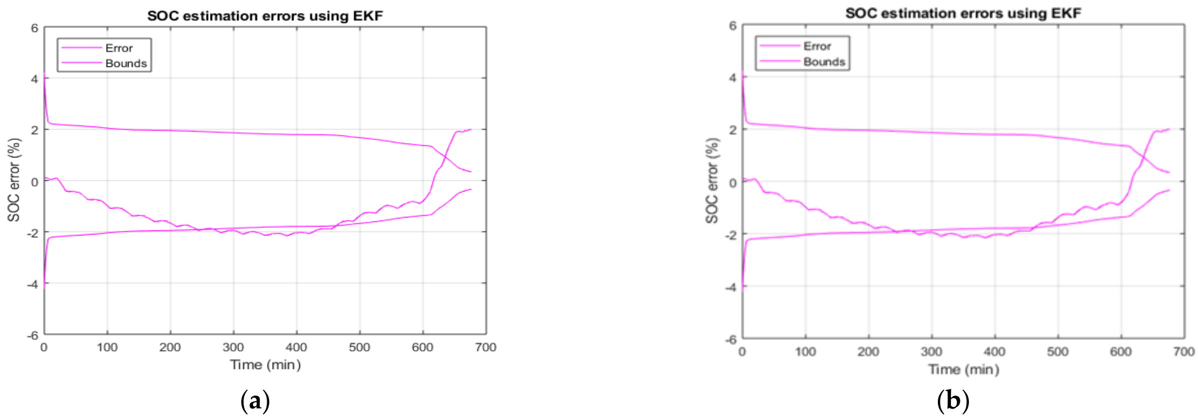

Figure 6. (**a**) SOC estimation using EKF; (**b**) SOC estimation error using EKF [101].

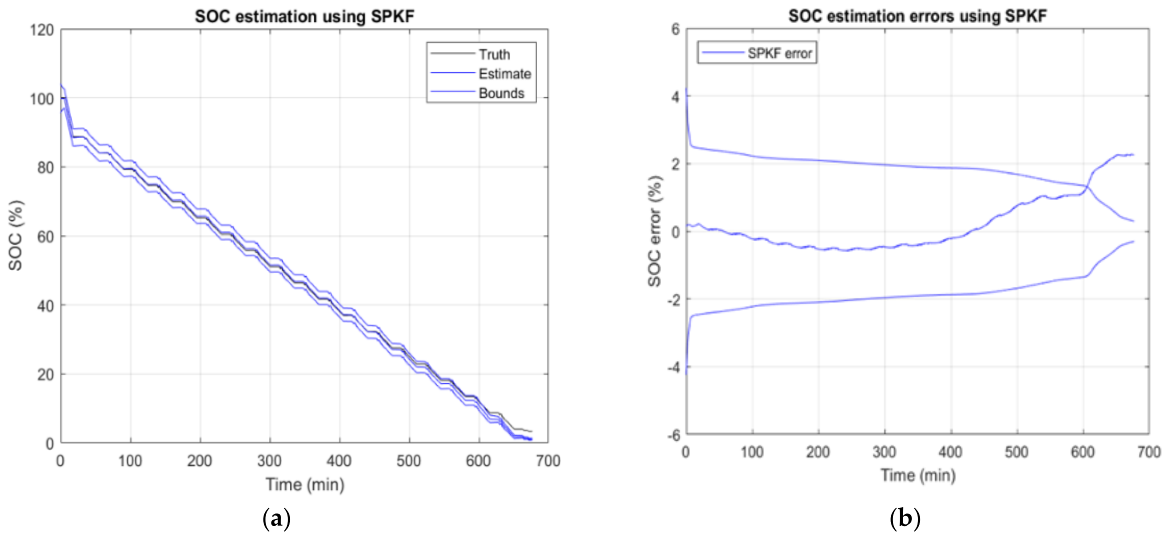

Figure 7. (**a**) SOC estimation using SPKF; (**b**) SOC estimation error using SPKF [101].

5.2. Performance Analysis of Kalman Filters

The comparison of various types of Kalman filters depends on different types of validation methods and load profiles. The estimation behavior and accuracy of algorithms are determined as a function of filter tuning parameters. The accuracy of the estimation of SOC and other states mainly depends on the number of RC networks and temperature. The correct parameter value of ECM is more critical than filter tuning parameters for the accuracy of KF. In a comparison of EKF, SPKF, and CKF, it was concluded that EKF had reduced accuracy but enhanced computational competence. Both CKF and SPKF are accurate (within 0.1% SOC error), but SPKF is not accurate in terms of lesser speed. Hence, CKF is most stable algorithm allowing a tradeoff between time consumption and accuracy [100]. EKF was compared and validated using the zero-hysteresis and hysteresis models. The EKF algorithm could not estimate the parameters of the hysteresis model due to it being dynamic over time. The DEKF algorithm was used for the hysteresis model rather than EKF to identify parameters and states of the system [102,103].

5.3. Issues, Challenges, and Future Directions

(1) The implementation of EC + KF in BMS for EVs has always been a challenging subject. KF provides a promising outlook for the high dynamic usage in HEVs and EVs. The crucial component of filter tuning is estimating the noise covariance matrix and the initialization of covariance matrices. The choice of these matrix parameters is crucial to making the perfect system.

(2) The most concerning issue is KF stability, which is achieved by reducing the special effects of the computational roundoff errors that lead to matrix asymmetry and a negative eigenvalue. This problem directly influences the Kalman gain that leads to the reduced speed of the convergence of the estimator at the time of computing the covariance matrix.

(3) KF requires a proper and accurate battery model to reduce the difficulties of estimating parameters. The modification of the algorithm is compulsory according to the application. A perfect controller is needed for all types of matrix multiplications.

6. BMS Algorithms for Non-Model-Based (Data-Driven Approach) State Estimation

It is challenging to directly observe the intricate chemical processes inside the battery. To ensure the safe and reliable operation of the battery management system, it is crucial to build an accurate mathematical model for the battery. A machine learning-based data cleaning technique is suitable for huge data in electric vehicle batteries. Machine learning- and deep learning-based models are becoming popular to achieve higher efficiency for state estimation of batteries in EV applications.

6.1. Lithium-Ion Battery Modeling Based on Big Data

Artificial intelligence techniques such as artificial neural networks and deep neural networks are progressive methods for estimating Li-ion battery states. Deep neural network methods have been used for SOC estimation. In Figure 8, the architecture of a deep neural network is displayed. The fuzzy neural network, recurrent neural network (RNN), feedforward neural network (FNN), backpropagation neural network (BPNN), long short-term memory (LSTM), LSTM-RNN, convolutional neural network (CNN), radial basis function neural network (RBF-NN), Gaussian process regression (GPR), and extreme learning machine (ELM) methods have been successfully implemented for the state estimation of Li-ion batteries in various studies [85–88]. In [89], an optimized deep fully convolutional network (FCN) with learning rate optimization was proposed, which showed superiority compared with RNN, LSTM, and GRU. Since machine learning techniques perform data mapping without considering the physical mechanism, abrupt errors can occasionally result. In [90], the proposed physics-constrained neural network (NN) simultaneously reduced both the physical constraint loss and the data mapping loss. The multioutput convolved Gaussian process (MCGP) was proposed for multitasking and transfer learning to use the latent function decomposition method for forecasting the capacity of battery cells [91].

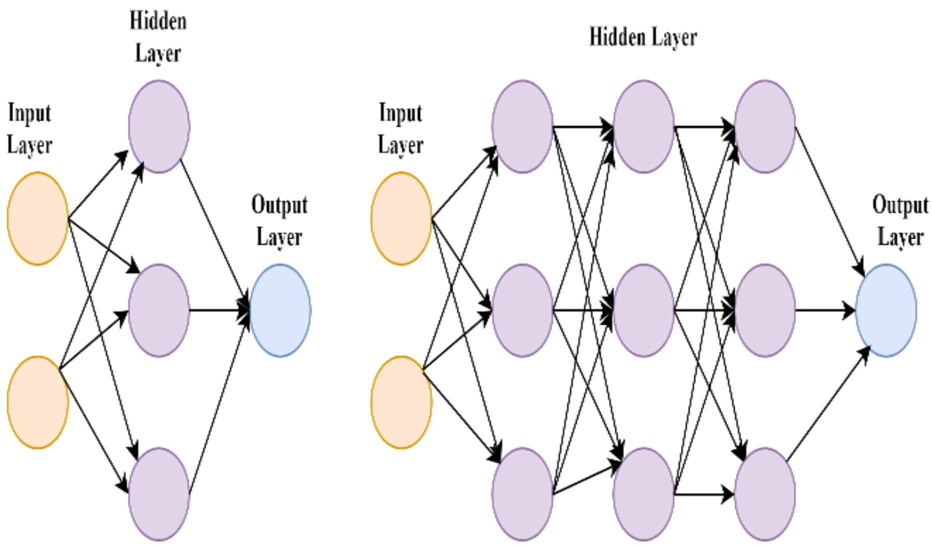

Figure 8. NN and deep neural network.

6.2. A simulation Comparison of Machine Learning Algorithms

The most conventional machine learning algorithms are regression, instance-based, regularization, decision tree, Bayesian, clustering, and association rule learning algorithms. On the basis of above classification, PyCaret was applied for model selection and fine-tuning to decide the best machine learning algorithms according to DST drive cycle data of NCR 18650B. A laboratory test was conducted to retrieve DST drive cycle data. Time, current, voltage, capacity, and SOC were measured with different temperatures. The PyCaret automation tool performed the simulation on DST drive cycle data (time, current, voltage, capacity, and SOC) to choose suitable ML algorithms for SOC estimation. The PyCaret automation tool came up with 21 algorithms (Table 6 gives the best SOC estimation solution for different drive cycle data on different Li-ion batteries. In Figure 9, the best algorithms among the 21 ML algorithms (random forest (RF), linear regression (LR), decision tree (DT), extra trees regressor (ETR), support vector regression (SVR), k neighbor regressor (KNN), extreme gradient boosting (EGB), and adaBoost (AB)) were chosen for SOC estimation according to accuracy, computation time, error rate, and performance. Non-model-based state estimation is reviewed in Table 7.

Table 6. A simulation comparison of ML algorithms with Pycaret automation tool on DST drive cycle dataset.

Sl No.	Model	MAE	MSE	RMSE	R^2	RMSLE	MAPE	TT (s)
1	Extra trees regressor	0.0026	0.0000	0.0052	0.9997	0.0037	−0.0260	0.1545
2	Extreme gradient boosting	0.0040	0.0000	0.0063	0.9996	0.0045	−0.0330	0.2134
3	Random forest	0.0034	0.0000	0.0066	0.9995	0.0047	−0.0312	0.2003
4	Light gradient boosting machine	0.0050	0.0001	0.0076	0.9994	0.0055	−0.0419	0.1213
5	Decision tree	0.0034	0.0001	0.0080	0.9993	0.0057	−0.0196	0.0104
6	Gradient boosting regressor	0.0034	0.0001	0.0080	0.9993	0.0057	−0.0196	0.0104
7	Adaboost regressor	0.0327	0.0016	0.0398	0.9835	0.0261	−0.4166	0.1861
8	Ridge regression	0.0272	0.0016	0.0400	0.9831	0.0325	−0.8945	0.0073
9	Least angle regression	0.0267	0.0016	0.0400	0.9831	0.0326	−0.9191	0.0059
10	Bayesian ridge	0.0267	0.0016	0.0400	0.9831	0.0326	−0.9190	0.0087
11	Linear regression	0.0267	0.0016	0.0400	0.9831	0.0326	−0.9191	0.0043
12	Random sample consensus	0.0257	0.0016	0.0401	0.9830	0.0329	−0.9936	0.1339
13	K neighbors regressor	0.0133	0.0017	0.0402	0.9819	0.0285	−0.0779	0.0072
14	Huber regressor	0.0251	0.0017	0.0414	0.9819	0.0341	−1.1640	0.0387
15	Theilsen regressor	0.0255	0.0018	0.0417	0.9816	0.0341	−1.1423	1.1475
16	Orthogonal matching pursuit	0.0472	0.0051	0.0708	0.9476	0.0512	−0.7833	0.0077
17	Passive aggressive regressor	0.0645	0.0053	0.0729	0.9448	0.0512	−0.4119	0.0076
18	Support vector machine	0.2675	0.0945	0.3074	0.0177	0.2126	−3.4891	0.2531
19	Lasso regression	0.2699	0.0959	0.3097	0.0032	0.2151	−3.7653	0.0094
20	Elastic net	0.2699	0.0959	0.3097	0.0032	0.2151	−3.7638	0.0068
21	Lasso least angle regression	0.2704	0.0964	0.3103	−0.001	0.2156	−3.7954	0.0062

MAE = mean average error, MSE = mean square error, RMSE = root-mean-square error; R^2 = Weber, RMSLE = volts, MAPE = seconds.

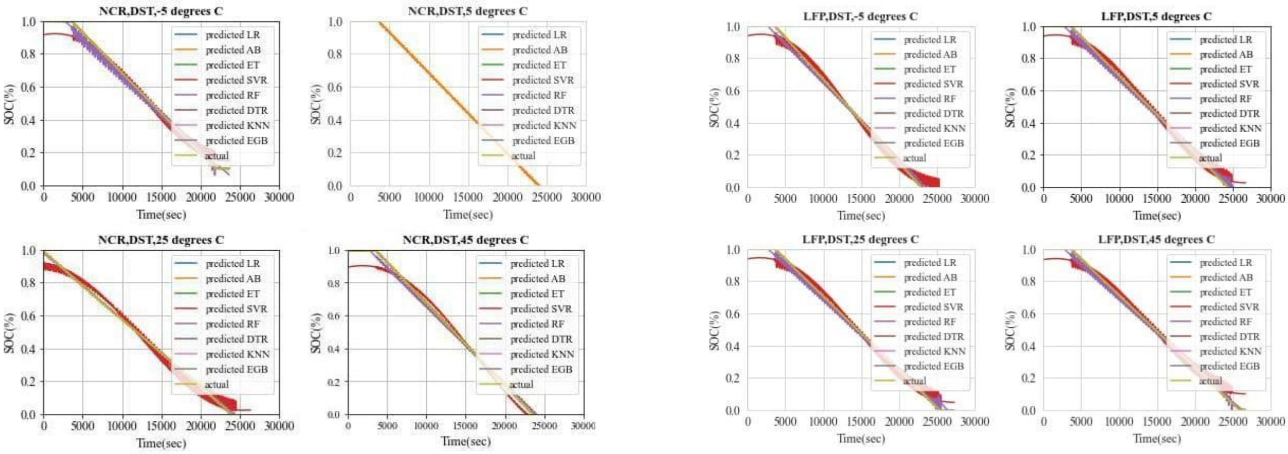

Figure 9. Comparison of ML algorithms for SOC estimation with different battery chemistry for DST drive cycle.

Table 7. Non-model-based online parameter and state estimation in he literature.

Ref.	Data-Driven Method	Battery Testing	RMSE/Error Rate (%)	Comparison	Online Parameters	Technical Comment
[94]	Deep transfer neural network + MDA (multiscale distribution adaptation)	BJDST, USO6, and FUDS	1.04	RNN, GRU, and LSTM	SOC	More robust than other methods
[104]	Deep neural network	DST, FUDS, BJDST, and US06	0.08	LSTM and CNN-GRU	SOC	Reduced error rate, Enhanced performance of SOC estimation
[105]	Recurrent Gaussian process regression (RGPR)	FUDS and US06	0.14	SVM, RVM, and NN	SOC	High accuracy, identification important input features
[106]	RNN (recurrent neural network) with gated recurrent unit	HWFET, LA92, UDDS, and US06	0.029	RNN	SOE	Energy prediction, range estimation
[107]	LSTM + GPR	Cycle test dataset	0.0032	GPR, LSTM, GPR + EMD, and LSTM + EMD (empirical mode decomposition)	RUL	Good adaptability, reliable, high certainty
[108]	Autoencoder + LSTM	DST and FUDS	0.72%, 0.90%, 1.30%	LSTM and RBFNN	SOC	Autoencoder is useful for optimum feature selection
[88]	Fuzzy neural network + form genetic algorithm	Charging/discharging		BPNN	SOC	High convergence rate
[87]	Extreme learning machine (ELM)–GSA (gravitational search algorithm)	DST, FUDS, and USO6	1.1%, 1.4%, 1.8%	Back propagation neural network (BPNN) and radial basis function neural network	SOC	Greater accuracy, low error
[109]	Feature selection + ML	Calce + NASA dataset		ELM and SVR	SOH	Accuracy, computational efficiency
[110]	Model + DNN metabolic gray model, multioutput Gaussian process regression	NEDS + UDDS + JP1015	±2	GPR and SVR	SOH + RUL	Great accuracy and robustness, closed-loop control, dynamic model
[111]	NN + EKF	Battery charging	3%	NN	SOC	Good prediction of SOC and fast convergence due to EKF RBF type NN taken to decide a suitable model for EKF
[112]	Fuzzy C-means	FUDS	1.68		SOC	The better initial value for optimization
[98]	LSTM + UKF	DST, US06, and FUDS	0.93	LSTM	SOC	Model-free, no need for OCV-SOC look-up table

Table 7. *Cont.*

Ref.	Data-Driven Method	Battery Testing	RMSE/Error Rate (%)	Comparison	Online Parameters	Technical Comment
[113]	NN	Charge/discharge	2.36%	EKF	SOC	Fast convergence speed, higher precision
[114]	Deep LSTM	Charge/discharge test	0.76%	LSTM-RNN	Capacity	DLSTM worked well with timeseries data Computationally fast
[115]	Bidirectional LSTM encoder–decoder	UDDS, LA92, US06, and HWFET	1.07%	LSTM-RNN and BSLTSM	SOC	Encoder and decoder architecture BSLSDM-ED can exhibit long-term dependencies from both past and future directions that estimate the accuracy of SOC
[116]	LSTM	HWFET, UDDS, LA92, and US06	1.606%	ECM	SOC	No need for modeling and an expansive filter
[89]	Deep convolution neural network	US06	0.85	LSTM, GRU, and CNN	SOC	Lowest RMSE compared to LSTM, GRU, and CNN, computationally competent, high speed, less cost
[117]	Stacked bidirectional LSTM	FUDS, US06, and BJDST	0.46	LSTM	SOC	Bidirectional LSTM works on both forward and backward sequential data to estimate SOC accurately
[79]	LSTM + ACKF	DST, US06, and FUDS	2.2, 4%	LSTM	SOC	Improved accuracy due to a combination of LSTM and ACKF
[118]	LSTM + SRCKF	DST and FUDS	0.4, 2%	LSTM	SOC	Better accuracy in the lower range of SOC
[119]	Radial basis function NN (RBFNN)	EV data	4%	ANN	Battery aging	Good choice for online BMS
[120]	SVR	DST	0.71, 6%, 0.4, 4%		SOC, Cell voltage	Quick SOC, worked well with low-cost BMS

As shown in Table 6, among all 21 algorithms, random forest, extreme gradient boosting, and extra trees regressor showed the best prediction results for the DST drive cycle in terms of MSE, MAE, and RMSE for state estimation of Li-ion batteries. In [92], random forest was used with differential search algorithm (DSA) optimization for SOC estimation for DST and FUDS cycles with an MAE of 0.193% and 0.346%, respectively. The above table provided a standard for comparing algorithms in terms of prediction error to choose an appropriate algorithm for EV applications. In [93], the SVM parameter was optimized using particle swarm optimization, and the prediction model error of the algorithm ranged from 1.65% to 2.5% according to cross-validation. The above table shows a 0.95% prediction error for the SVM algorithm using cross-validation.

6.3. Issues, Challenges, and Future Directions

- Issues and Challenges

(1) The key issue is to develop a hierarchical model with a powerful feature extraction method for the estimation of SOH.

(2) The difficulties in training and optimizing parameters in DL are due to gradient descent in the nonconvex problem space.

(3) The transfer learning should be more robust to changes in data features and heterogeneous data.

(4) The most important challenge of probabilistic methods is computation time.

- Future trends

(1) The deep learning network faces challenges due to the limitation of backpropagation-based training. The metaheuristic algorithm can be applied to train DL networks to overcome this limitation.

(2) The training time plays a significant role in the success of DL algorithms. Monte Carlo sampling can be used to select smaller but critical data to decrease the training time of networks.

(3) Effective feature extraction from battery data is the future trend in non-model-based estimation. Multiple deep learning networks instead of single algorithms should be used for feature extraction.

(4) Probability forecasting models based on DL have a prominent future in timeseries data due to their ability to measure uncertainties.

7. Fault Diagnosis and the State of Balance

7.1. Research Challenges and Advances in Series and Parallel Connection (Battery Pack)

EV applications require high power (P = VI) to provide high current and voltage. The topology of the pack must be decided before implementation with the voltage range and peak current estimation. Series-connected cells are required for low-energy high-power applications, whereas parallel-connected cells are chosen for the high-energy applications. Active and passive balancing is used for balancing series-connected battery packs to control the overcharge and over-discharge of the battery pack. Cells with the same initial state and parameters experience the same current in series connection. Some simulation results explained the research challenges for series- and parallel-connected battery packs [43].

Various studies focused on series-connected cell balancing techniques and applications [10,36]. Simulation results are shown in Figure 10a,b, where eight cells were connected in series and three series-connected modules in a pack were connected in parallel. The simulation showed that all cells experienced the same current because of series connection in the same series-connected modules, but different modules experienced different currents. Here, we can also observe that cells were not balanced in series-connected modules. Cell voltages were not the same, but the overall voltage of the three series-connected modules was identical. Therefore, cell balancing is needed for battery pack modules connected in series.

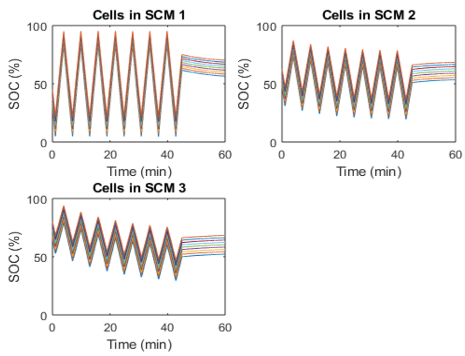

(a)

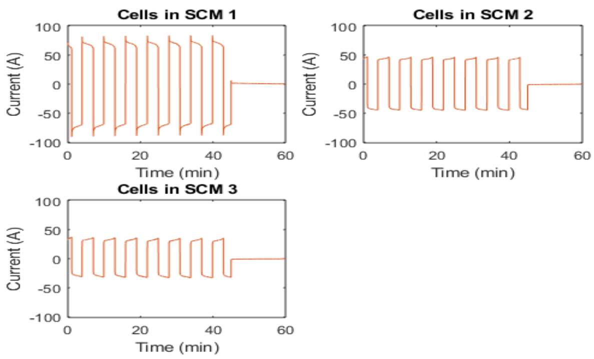

(b)

Figure 10. (**a**) Simulation results of SOC of SCM. (**b**) Simulation results of the current SCM. Adopted from [101].

The cells had dissimilar SOCs due to varying resistances and capacities during cycling in a parallel-connected cell. In Figure 11a, the simulation results show different SOC values for different cells (shown by a different color) while cycling, but they reached the same value at the time of rest. Here, we can observe that, in parallel-connected modules, the cell balanced itself. Due to varying resistance, the current experienced by individual cells, as shown in Figure 11b in a PCM, can be completely different from each other. When the applied battery-pack current is zero, it does not mean that the cell current is also zero because the cells may have an unequal state of charge, causing circulating balancing currents because of the parallel electrical connections of cells within a PCM. Different types of cell equalization techniques have been discussed in various studies [10,121]. The advancement of hardware systems with a control strategy/algorithm is compulsory for cell equalizer circuits [122]. The development of an algorithm to control hardware system cell equalization is a crucial task [123]. Centralized, modular, and distributed controllers are mainly used to control the balancer circuit. In [124], fuzzy logic control was used to manage parallel-connected cells. Model predictive control is also a very accurate advanced technology where the accuracy of the cell mathematical model correlates with the cell equalizer [125].

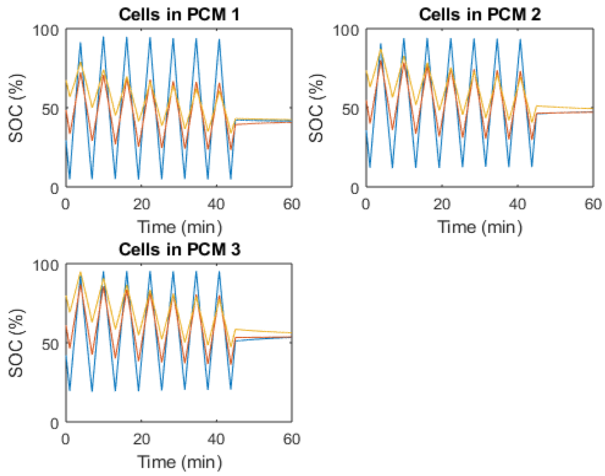

(**a**)

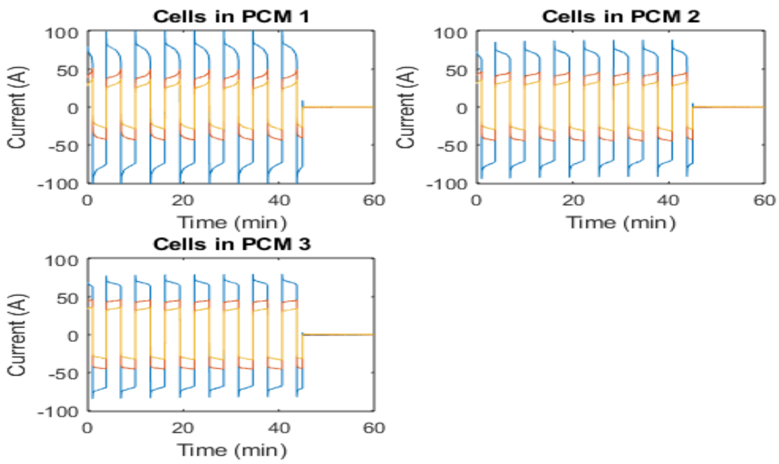

(**b**)

Figure 11. (**a**) Simulation of SOC of PCM. (**b**) Simulation of current distribution in PCM. Adopted from [101].

7.2. Mode-l and Non-Model-Based Fault Diagnosis and State of Safety of Li-Ion Battery

Li-ion battery fault diagnosis is a vital issue in the BMS of electric vehicles for state of safety (SOS) estimation. Overvoltage, under-voltage, overheating, loose connection, insulation, external short-circuit, internal short-circuit, open circuit, and sensor failure occur under Li-ion battery fault conditions, which accelerate aging, degradation, and thermal runway [126]. Fault diagnosis is challenging due to complex nonlinear time-varying internal states of Li-ion batteries or packs with inconsistency [4]. The voltage differences in series-connected cells and current inconsistencies in parallel-connected cells cause many types of faults within the battery pack. The preprocessing step for FD is based on the accuracy of feature selection. Model-based filters and observers, signal processing-based methods, and machine learning-based methods are the most popular feature extraction methods [127] (Figure 12). Signal processing methods use the entropy or correlation coefficient as a fault parameter to measure signals and any irregularities in these parameters. In [128], model-based battery fault diagnosis was proposed to enable joint soft SC fault estimate and detection. An H-infinity nonlinear observer was built to track changes in model parameters on the basis of an enhanced estimate of the state of charge (SOC) and soft SC current in the presence of a space battery model. For accelerated aging diagnosis of lithium-ion batteries, an integrated framework of aging mechanisms and data-driven techniques (IFAMDM) was introduced [128]. Some studies suggested a wavelet-based method for defect discovery in lithium-ion batteries to ensure the dependability and safety of electric vehicles [129]. Modified sample entropy was used for real-time multi-fault diagnosis of early battery failure [130]. In [131], feature engineering techniques and artificial intelligence (AI) algorithms (including machine learning, neural networks, and deep learning) in condition monitoring and problem detection approaches were extensively summarized. Fault diagnosis algorithms are reviewed in Table 8.

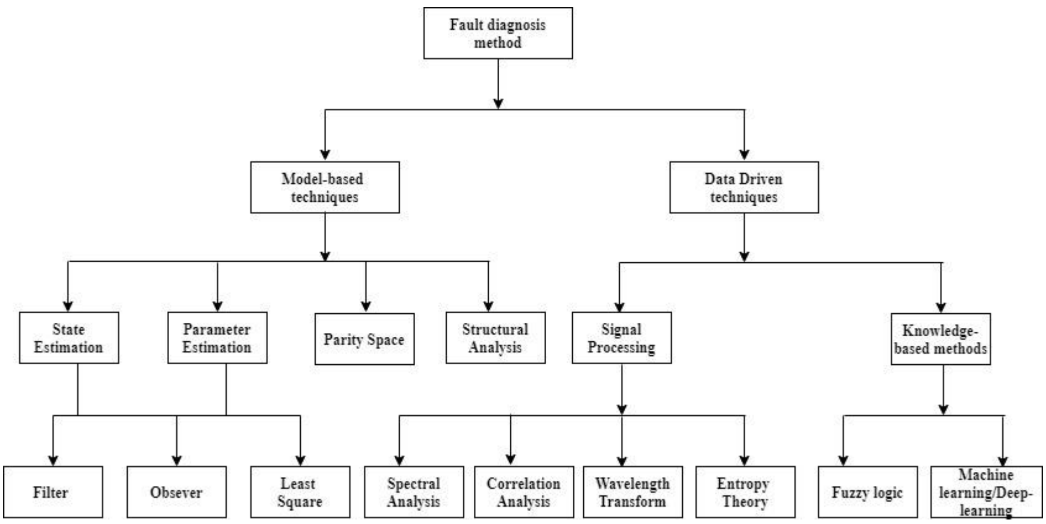

Figure 12. Classification of algorithms for LiB fault diagnosis [14,63].

Table 8. Algorithm comparisons of battery fault diagnosis.

Diagnostic Techniques	Battery Faults	Benefit	Drawback	Limitations	References
RLS Filter	ISC (Internal short circuit) MSC (micro-short circuit)	Simple, low cost, and complexity	Model-based ambiguity and minimal estimation accuracy of states	Need information about other series and parallel connected cell leads to inconsistency and balancing	[132]
SVM	Connection fault	Identify the severity of voltage fault with the time	Cannot identify current working state for big and high dimension data	Suitable only for small, simple data	[133]
RLS-UKF	Sensor fault detection	More accurate and less prediction time for a current sensor	Longer time for prediction of fault due to voltage sensor	Limitation of Gaussian white noise	[134]

Table 8. *Cont.*

Diagnostic Techniques	Battery Faults	Benefit	Drawback	Limitations	References
AEKF	overcharge and over-discharge faults	Adaptive model-based technique	Model-based limitation for parameters and states estimation	Required to generate a residual signal	[135]
Neural Network	Fault due to the voltage sensor	Identify abnormal voltage data	required big historical data	Overfitting	[136]
Statistical method	Diagnosis of the real-time fault with the time	Identify the future fault	Need large history data	Overfitting	[126]
Entropy Theory	Short circuit	Fast diagnosis of the short circuit	Vulnerable to measurement noise	Failed in considerable inconsistency and with varied temperature and the current rate	[130]
DEKF	Sensor fault	Estimate accurately continuous state and parameter	complexity	computational cost	[137]
LSTM	Thermal runaway	Increase accuracy, decrease computational time	Increase complexity by coupling model and data-driven method	Failed when voltage within is within the set threshold	[138]
WAVELET	Diagnosis real voltage value	Noise removal from the real voltage	Affected by the set value of interval parameters	Cross-voltage test	[129]
Correlation method	Short circuit	Robust for real-time application	Irregular voltage drops	Vulnerable to measurement noise	[139]
Neural network	Thermal Fault	Stretch forward technique and residual monitor used for identifying fault	Slow fault and long-term degradation require to be enhanced	Only work on big historical data	[140]

7.3. Issues, Challenges, and the Future Trend of Online Fault Diagnosis

- Issues and Challenges

(1) A realistic mathematical model for fault diagnosis to characterize the fault of LiBs should be established. It is still difficult to monitor the internal state of the battery and the coupling of faults.

(2) The verification of the fault threshold is not robust in model-based fault diagnosis. The capacity degradation of LiBs also influences the accuracy of the threshold; therefore, its needs to be adjusted with the battery's cycle life, rather than being fixed. The adaptive threshold can resolve this issue, but further research in this area needs to be done.

(3) Fault-tolerant control for BMS needs to be researched to detect the ISC and ESC faults.

(4) The battery sensors and actuators are supposed to be fault-free in the FD system; therefore, multi-fault detection is a very difficult issue in this area.

(5) Very few studies investigated current distribution within parallel-connected cells and its effect on the safety, lifetime, and power of the cell for EV applications; furthermore, their experimental setup has not been explained.

- Future trends

(1) Data-driven methods show good prospects to develop the fault diagnosis of LiB battery systems; however, due to the limitation of a single method to meet the desired demand, the overall efficiency can be achieved through the fusion of multiple FD algorithms.

(2) The model-based FD method can be improved by detecting early faults, model uncertainties, and noises.

(3) Fault-tolerant control (FTC) should be designed as a robust controller to recognize faults and adjust control accordingly.

8. Conclusions

In this paper, the development of algorithms for online BMS was reviewed with a focus on key issues, limitations, challenges, and future directions. The development of model-based algorithms is more accurate and robust but suffers from a higher computational time and complexity. Filters and observers require battery modeling and parameter fitting in the battery model. Nonlinear observers and filters need to be more robust to intermittent and time-delayed observations. Data-driven-based algorithm development does not require extensive domain knowledge and computation time, unlike model-based algorithm development. However, data-driven methods require a large amount of data, which is a big drawback. The development of algorithms for combined estimation on different timescales of various states of LiBs is needed to make BMSs more robust and efficient. The performance of algorithms depends on hyperparameters in deep learning networks, which can be optimized using meta-heuristics methods. The fusion of model- and non-model-based techniques is currently a research hotspot as it combines the advantages of different types of algorithms and models to solve complex problems. The data-driven approach for multisource battery safety condition monitoring and unknown multi-fault diagnosis is an active area of research in EV applications. Deep learning can also be utilized for closed-loop optimization of fast charging for EVs. Hardware in loop (HIL) and rapid prototyping (RP) simulations support the control algorithms under different operating and fault conditions for automatic code generation. Automatic code generation can make required changes in proposed algorithms to obtain an optimal solution of BMSs. Code generation can be incorporated into the workflow standard of xEV. In general, model- and non-model-based algorithms focus on the challenges caused by software complexity in BMS. Interactions with control hardware to change algorithm parameters and test data can provide an optimal solution for online BMSs. The present article can certainly help to develop methods for the future generation of online BMSs for EV applications.

Author Contributions: Conceptualization, data curation, formal analysis, investigation, software, validation, N.B.; Supervision, resources, project administration, S.M. and K.S.T.; Supervision, project administration, writing—review & editing, M.S. (Mohamed Shaaban); Funding acquisition, writing—review & editing, M.S. (Mehdi Seyedmahmoudian) and A.S. All authors have read and agreed to the published version of the manuscript.

Funding: This research received no external funding.

Institutional Review Board Statement: Not applicable.

Informed Consent Statement: Not applicable.

Conflicts of Interest: The authors declare no conflict of interest.

Nomenclature

AB	Adaboost
AEKF	Adaptive extended Kalman filter
AHC	Ampere-hour counting
AM	Analytical models
ANN	Artificial neural network
AR	Auto-regression
ARIMA	Autoregressive integrated moving average
BLSTM	Deep long short-term memory
BMS	Battery management system
CC-CV	Constant current–constant voltage
CDKF	Central difference Kalman filter

CNN	Convolution neural network
CP-CV	Constant power–constant voltage
CPE	Constant phase element
CVA	Canonical variate analysis
DBN	Deep belief network
DBNN	Deep belief neural network
DCNN	Deep convolution neural network
DD	Data-driven
DEKF	Dual extended Kalman filter
DL	Deep learning
DNN	Deep neural netowrk
DST	Dynamic stress test
DT	Decision tree
ECM	Equivalent circuit model
EECM	Electrical equivalent circuit models
EGB	Extreme gradient boosting
EIS	Electrochemical impedance spectroscopy
EKF	Extended Kalman filter
EMD	Empirical mode decomposition
ESC	Enhanced self-correcting
ETM	Electro-thermal modeling
ETR	Extra trees regressor
EV	Electric vehicle
FA	Firefly algorithm
FCN	Fully convolutional network
FOM	Fractional-order model
FUDS	Federal urban driving schedule
GA	Genetic algorithm
GPR	Gaussian process regression
HPPC	Hybrid pulse power characterization
HEVs	Hybrid electric vehicles
IIR	Infinite impulse response
KNN	K neighbor regressor
LCO	Lithium cobalt oxide
LFP	Lithium iron phosphate
LiBs	Lithium-ion batteries
LMO	Lithium manganese oxide
LR	Linear regression
LSTM	Long short-term memory
LTO	Lithium titanate oxide
MAE	Mean absolute error
ML	Machine learning
MSE	Mean square error
NCA	Lithium nickel cobalt aluminum oxide
NMC	Lithium nickel manganese cobalt oxide
OCV	Open-circuit voltage
ODEs	Ordinary differential equations
PDEs	Partial differential equations
PHEVs	Plug-in hybrid electric vehicle
PNGV	Partnership new generation of vehicle
PSO	Partical swam optimization
RF	Random forest
RMSE	Root-mean-square error
RNN	Recurrent neural network
RUL	Remaining userful life
SAA	Simulated annealing algorithm
SAE	Stacked auto encoder
LS	Lebesgue sampling

RS	Riemann sampling
SMO	Sliding mode observer
SOC	State of charge
SOE	State of energy
SOF	State of function
SOH	State of health
SOP	State of power
SOS	State of safety
SOT	State of temperature
SPKF	Sigma point Kalman filter
SVR	Support vector regression
TM	Thermal model
UDDS	Urban dynamometer driving schedule
UKF	Unscented Kalman filter
WD	Wavelet decomposition

References

1. Nykvist, B.; Nilsson, M. Rapidly falling costs of battery packs for electric vehicles. *Nat. Clim. Chang.* **2015**, *5*, 329–332. [CrossRef]
2. Sulaiman, N.; Hannan, M.; Mohamed, A.; Majlan, E.; Daud, W.W. A review on energy management system for fuel cell hybrid electric vehicle: Issues and challenges. *Renew. Sustain. Energy Rev.* **2015**, *52*, 802–814. [CrossRef]
3. Hannan, M.A.; Hoque, M.D.M.; Hussain, A.; Yusof, Y.; Ker, A.P.J. State-of-the-Art and Energy Management System of Lithium-Ion Batteries in Electric Vehicle Applications: Issues and Recommendations. *IEEE Access Spec. Sect. Adv. Energy Storage Technol. Appl.* **2018**, *6*, 19362–19378. [CrossRef]
4. Xiong, R.; Sun, W.; Yu, Q.; Sun, F. Research progress, challenges and prospects of fault diagnosis on battery system of electric vehicles. *Appl. Energy* **2020**, *279*, 115855. [CrossRef]
5. Yong, J.Y.; Ramachandaramurthy, V.K.; Tan, K.M.; Mithulananthan, N. A review on the state-of-the-art technologies of electric vehicle, its impacts and prospects. *Renew. Sustain. Energy Rev.* **2015**, *49*, 365–385. [CrossRef]
6. Lin, Q.; Wang, J.; Xiong, R.; Shen, W.; He, H. Towards a smarter battery management system: A critical review on optimal charging methods of lithium ion batteries. *Energy* **2019**, *183*, 220–234. [CrossRef]
7. Nejad, S.; Gladwin, D.; Stone, D. A systematic review of lumped-parameter equivalent circuit models for real-time estimation of lithium-ion battery states. *J. Power Sources* **2016**, *316*, 183–196. [CrossRef]
8. Shrivastava, P.; Soon, T.K.; Bin Idris, M.Y.I.; Mekhilef, S. Overview of model-based online state-of-charge estimation using Kalman filter family for lithium-ion batteries. *Renew. Sustain. Energy Rev.* **2019**, *113*, 109233. [CrossRef]
9. Hu, X.; Feng, F.; Liu, K.; Zhang, L.; Xie, J.; Liu, B. State estimation for advanced battery management: Key challenges and future trends. *Renew. Sustain. Energy Rev.* **2019**, *114*, 109334. [CrossRef]
10. Das, U.K.; Shrivastava, P.; Tey, K.S.; Bin Idris, M.Y.I.; Mekhilef, S.; Jamei, E.; Seyedmahmoudian, M.; Stojcevski, A. Advancement of lithium-ion battery cells voltage equalization techniques: A review. *Renew. Sustain. Energy Rev.* **2020**, *134*, 110227. [CrossRef]
11. Liu, K.; Ashwin, T.R.; Hu, X.; Lucu, M.; Widanage, W.D. An evaluation study of different modelling techniques for calendar ageing prediction of lithium-ion batteries. *Renew. Sustain. Energy Rev.* **2020**, *131*, 110017. [CrossRef]
12. Hannan, M.A.; Lipu, M.S.H.; Hussain, A.; Mohamed, A. A review of lithium-ion battery state of charge estimation and management system in electric vehicle applications: Challenges and recommendations. *Renew. Sustain. Energy Rev.* **2017**, *78*, 834–854. [CrossRef]
13. Lu, L.; Han, X.; Li, J.; Hua, J.; Ouyang, M. A review on the key issues for lithium-ion battery management in electric vehicles. *J. Power Sources* **2013**, *226*, 272–288. [CrossRef]
14. Tran, M.-K.; Fowler, M. A Review of Lithium-Ion Battery Fault Diagnostic Algorithms: Current Progress and Future Challenges. *Algorithms* **2020**, *13*, 62. [CrossRef]
15. Jin, G.; Li, L.; Xu, Y.; Hu, M.; Fu, C.; Qin, D. Comparison of SOC Estimation between the Integer-Order Model and Fractional-Order Model Under Different Operating Conditions. *Energies* **2020**, *13*, 1785. [CrossRef]
16. Naseri, F.; Schaltz, E.; Stroe, D.-I.; Gismero, A.; Farjah, E. An Enhanced Equivalent Circuit Model With Real-Time Parameter Identification for Battery State-of-Charge Estimation. *IEEE Trans. Ind. Electron.* **2021**, *69*, 3743–3751. [CrossRef]
17. Bian, X.; Wei, Z.; He, J.; Yan, F.; Liu, L. A Two-Step Parameter Optimization Method for Low-Order Model-Based State-of-Charge Estimation. *IEEE Trans. Transp. Electrif.* **2020**, *7*, 399–409. [CrossRef]
18. Severson, K.A.; Attia, P.M.; Jin, N.; Perkins, N.; Jiang, B.; Yang, Z.; Chen, M.H.; Aykol, M.; Herring, P.K.; Fraggedakis, D.; et al. Data-driven prediction of battery cycle life before capacity degradation. *Nat. Energy* **2019**, *4*, 383–391. [CrossRef]
19. Wang, S.; Kuang, K.; Han, X.; Chu, Z.; Lu, L.; Ouyang, M. A model-based continuous differentiable current charging approach for electric vehicles in direct current microgrids. *J. Power Sources* **2021**, *482*, 229019. [CrossRef]
20. Behi, H.; Karimi, D.; Kalogiannis, T.; He, J.; Patil, M.S.; Muller, J.-D.; Haider, A.; Van Mierlo, J.; Berecibar, M. Advanced hybrid thermal management system for LTO battery module under fast charging. *Case Stud. Therm. Eng.* **2022**, *33*, 101938. [CrossRef]

21. Wang, Y.; Zhao, G.; Zhou, C.; Li, M.; Chen, Z. Lithium-Ion Battery Optimal Charging using Moth-flame Optimization Algorithm and Fractional-Order Model. *IEEE Trans. Transp. Electrif.* **2022**, 1. [CrossRef]
22. Faria, J.P.D.; Velho, R.L.; Calado, M.R.A.; Pombo, J.A.N.; Fermeiro, J.B.L.; Mariano, S.J.P.S. A New Charging Algorithm for Li-Ion Battery Packs Based on Artificial Neural Networks. *Batteries* **2022**, *8*, 18. [CrossRef]
23. Shen, W.; Vo, T.T.; Kapoor, A. Charging algorithms of lithium-ion batteries: An overview. In Proceedings of the 2012 7th IEEE Conference on Industrial Electronics and Applications (ICIEA), Singapore, 18–20 July 2012; pp. 1567–1572. [CrossRef]
24. Zhang, S.S. The effect of the charging protocol on the cycle life of a Li-ion battery. *J. Power Sources* **2006**, *161*, 1385–1391. [CrossRef]
25. Liu, Y.-H.; Hsieh, C.-H.; Luo, Y.-F. Search for an Optimal Five-Step Charging Pattern for Li-Ion Batteries Using Consecutive Orthogonal Arrays. *IEEE Trans. Energy Convers.* **2011**, *26*, 654–661. [CrossRef]
26. Wang, S.-C.; Liu, Y.-H. A PSO-Based Fuzzy-Controlled Searching for the Optimal Charge Pattern of Li-Ion Batteries. *IEEE Trans. Ind. Electron.* **2014**, *62*, 2983–2993. [CrossRef]
27. Chen, L.-R. Design of Duty-Varied Voltage Pulse Charger for Improving Li-Ion Battery-Charging Response. *IEEE Trans. Ind. Electron.* **2008**, *56*, 480–487. [CrossRef]
28. Khan, A.B.; Choi, W. Optimal Charge Pattern for the High-Performance Multistage Constant Current Charge Method for the Li-Ion Batteries. *IEEE Trans. Energy Convers.* **2018**, *33*, 1132–1140. [CrossRef]
29. Li, Y.; Li, K.; Xie, Y.; Liu, J.; Fu, C.; Liu, B. Optimized charging of lithium-ion battery for electric vehicles: Adaptive multistage constant current–constant voltage charging strategy. *Renew. Energy* **2019**, *146*, 2688–2699. [CrossRef]
30. Vo, T.T.; Chen, X.; Shen, W.; Kapoor, A. New charging strategy for lithium-ion batteries based on the integration of Taguchi method and state of charge estimation. *J. Power Sources* **2015**, *273*, 413–422. [CrossRef]
31. Liu, Y.-H.; Teng, J.-H.; Lin, Y.-C. Search for an Optimal Rapid Charging Pattern for Lithium–Ion Batteries Using Ant Colony System Algorithm. *IEEE Trans. Ind. Electron.* **2005**, *52*, 1328–1336. [CrossRef]
32. Notten, P.; Veld, J.O.H.; van Beek, J. Boostcharging Li-ion batteries: A challenging new charging concept. *J. Power Sources* **2005**, *145*, 89–94. [CrossRef]
33. Keil, P.; Jossen, A. Charging protocols for lithium-ion batteries and their impact on cycle life—An experimental study with different 18650 high-power cells. *J. Energy Storage* **2016**, *6*, 125–141. [CrossRef]
34. Tar, B.; Fayed, A. An overview of the fundamentals of battery chargers. In Proceedings of the 2016 IEEE 59th International Midwest Symposium on Circuits and Systems (MWSCAS), Abu Dhabi, United Arab Emirates, 16–19 October 2016; pp. 1–4. [CrossRef]
35. Chen, L.-R. A Design of an Optimal Battery Pulse Charge System by Frequency-Varied Technique. *IEEE Trans. Ind. Electron.* **2007**, *54*, 398–405. [CrossRef]
36. Cho, I.-H.; Lee, P.-Y.; Kim, J.-H. Analysis of the Effect of the Variable Charging Current Control Method on Cycle Life of Li-ion Batteries. *Energies* **2019**, *12*, 3023. [CrossRef]
37. Chen, L.-R.; Wu, S.-L.; Shieh, D.-T.; Chen, T.-R. Sinusoidal-Ripple-Current Charging Strategy and Optimal Charging Frequency Study for Li-Ion Batteries. *IEEE Trans. Ind. Electron.* **2012**, *60*, 88–97. [CrossRef]
38. Abdel-Monem, M.; Trad, K.; Omar, N.; Hegazy, O.; Mantels, B.; Mulder, G.; Van den Bossche, P.; Van Mierlo, J. Lithium-ion batteries: Evaluation study of different charging methodologies based on aging process. *Appl. Energy* **2015**, *152*, 143–155. [CrossRef]
39. Abdel-Monem, M.; Trad, K.; Omar, N.; Hegazy, O.; Bossche, P.V.D.; Van Mierlo, J. Influence analysis of static and dynamic fast-charging current profiles on ageing performance of commercial lithium-ion batteries. *Energy* **2017**, *120*, 179–191. [CrossRef]
40. Tomaszewska, A.; Chu, Z.; Feng, X.; O'Kane, S.; Liu, X.; Chen, J.; Ji, C.; Endler, E.; Li, R.; Liu, L.; et al. Lithium-ion battery fast charging: A review. *eTransportation* **2019**, *1*, 100011. [CrossRef]
41. Patnaik, L.; Praneeth, A.V.J.S.; Williamson, S.S. A Closed-Loop Constant-Temperature Constant-Voltage Charging Technique to Reduce Charge Time of Lithium-Ion Batteries. *IEEE Trans. Ind. Electron.* **2018**, *66*, 1059–1067. [CrossRef]
42. Marcis, V.A.; Praneeth, A.; Patnaik, L.; Williamson, S.S. Analysis of CT-CV Charging Technique for Lithium-ion and NCM 18650 Cells. In Proceedings of the 2020 IEEE International Conference on Power Electronics, Smart Grid and Renewable Energy (PESGRE2020), Cochin, India, 2–4 January 2020; pp. 1–6. [CrossRef]
43. Plett, G.L. Dr. Gregory L. Plett's Homepage. Available online: http://mocha-java.uccs.edu/ (accessed on 8 July 2020).
44. Wang, Y.; Li, J.; Zhang, J.; Pecht, M. Lithium-iron-phosphate battery electrochemical modelling under a wide range of ambient temperatures. *J. Electroanal. Chem.* **2021**, *882*, 115041. [CrossRef]
45. Ngandjong, A.C.; Lombardo, T.; Primo, E.N.; Chouchane, M.; Shodiev, A.; Arcelus, O.; Franco, A.A. Investigating electrode calendering and its impact on electrochemical performance by means of a new discrete element method model: Towards a digital twin of Li-Ion battery manufacturing. *J. Power Sources* **2020**, *485*, 229320. [CrossRef]
46. Gao, Y.; Liu, C.; Chen, S.; Zhang, X.; Fan, G.; Zhu, C. Development and parameterization of a control-oriented electrochemical model of lithium-ion batteries for battery-management-systems applications. *Appl. Energy* **2022**, *309*, 118521. [CrossRef]
47. Lai, X.; Zheng, Y.; Sun, T. A comparative study of different equivalent circuit models for estimating state-of-charge of lithium-ion batteries. *Electrochim. Acta* **2018**, *259*, 566–577. [CrossRef]
48. Seaman, A.; Dao, T.-S.; McPhee, J. A survey of mathematics-based equivalent-circuit and electrochemical battery models for hybrid and electric vehicle simulation. *J. Power Sources* **2014**, *256*, 410–423. [CrossRef]
49. Yang, Z.; Patil, D.; Fahimi, B. Electrothermal Modeling of Lithium-Ion Batteries for Electric Vehicles. *IEEE Trans. Veh. Technol.* **2018**, *68*, 170–179. [CrossRef]

50. Mesbahi, T.; Rizoug, N.; Bartholomeus, P.; Sadoun, R.; Khenfri, F.; Le Moigne, P. Dynamic Model of Li-Ion Batteries Incorporating Electrothermal and Ageing Aspects for Electric Vehicle Applications. *IEEE Trans. Ind. Electron.* **2017**, *65*, 1298–1305. [CrossRef]
51. Huria, T.; Ceraolo, M.; Gazzarri, J.; Jackey, R. High fidelity electrical model with thermal dependence for characterization and simulation of high-power lithium battery cells. In Proceedings of the 2012 IEEE International Electric Vehicle Conference, Greenville, SC, USA, 4–8 March 2012.
52. Lai, X.; Wang, S.; Ma, S.; Xie, J.; Zheng, Y. Parameter sensitivity analysis and simplification of equivalent circuit model for the state of charge of Lithium-Ion batteries. *Electrochim. Acta* **2019**, *330*, 135239. [CrossRef]
53. Shen, P.; Ouyang, M.; Lu, L.; Li, J.; Feng, X. The Co-estimation of State of Charge, State of Health, and State of Function for Lithium-Ion Batteries in Electric Vehicles. *IEEE Trans. Veh. Technol.* **2017**, *67*, 92–103. [CrossRef]
54. Tran, M.-K.; Mevawala, A.; Panchal, S.; Raahemifar, K.; Fowler, M.; Fraser, R. Effect of integrating the hysteresis component to the equivalent circuit model of Lithium-ion battery for dynamic and non-dynamic applications. *J. Energy Storage* **2020**, *32*, 101785. [CrossRef]
55. Miniguano, H.; Barrado, A.; Lazaro, A.; Zumel, P.; Fernandez, C. General Parameter Identification Procedure and Comparative Study of Li-Ion Battery Models. *IEEE Trans. Veh. Technol.* **2019**, *69*, 235–245. [CrossRef]
56. Lai, X.; Gao, W.; Zheng, Y.; Ouyang, M.; Li, J.; Han, X.; Zhou, L. A comparative study of global optimization methods for parameter identification of different equivalent circuit models for Li-ion batteries. *Electrochim. Acta* **2018**, *295*, 1057–1066. [CrossRef]
57. Zou, C.; Hu, X.; Dey, S.; Zhang, L.; Tang, X. Nonlinear Fractional-Order Estimator with Guaranteed Robustness and Stability for Lithium-Ion Batteries. *IEEE Trans. Ind. Electron.* **2017**, *65*, 5951–5961. [CrossRef]
58. Tian, J.; Xiong, R.; Yu, Q. Fractional-Order Model-Based Incremental Capacity Analysis for Degradation State Recognition of Lithium-Ion Batteries. *IEEE Trans. Ind. Electron.* **2018**, *66*, 1576–1584. [CrossRef]
59. Xiong, R.; Tian, J.; Shen, W.; Sun, F. A Novel Fractional Order Model for State of Charge Estimation in Lithium Ion Batteries. *IEEE Trans. Veh. Technol.* **2018**, *68*, 4130–4139. [CrossRef]
60. Wei, Y.; Ling, L. State-of-Charge Estimation for Lithium-Ion Batteries Based on Temperature-Based Fractional-Order Model and Dual Fractional-Order Kalman Filter. *IEEE Access* **2022**, *10*, 37131–37148. [CrossRef]
61. Wu, J.; Fang, C.; Jin, Z.; Zhang, L.; Xing, J. A multi-scale fractional-order dual unscented Kalman filter based parameter and state of charge joint estimation method of lithium-ion battery. *J. Energy Storage* **2022**, *50*, 104666. [CrossRef]
62. Zou, C.; Zhang, L.; Hu, X.; Wang, Z.; Wik, T.; Pecht, M. A review of fractional-order techniques applied to lithium-ion batteries, lead-acid batteries, and supercapacitors. *J. Power Sources* **2018**, *390*, 286–296. [CrossRef]
63. Hu, X.; Zhang, K.; Liu, K.; Lin, X.; Dey, S.; Onori, S. Advanced Fault Diagnosis for Lithium-Ion Battery Systems: A Review of Fault Mechanisms, Fault Features, and Diagnosis Procedures. *IEEE Ind. Electron. Mag.* **2020**, *14*, 65–91. [CrossRef]
64. Hossain, M.; Haque, E.; Arif, M.T. Online Model Parameter and State of Charge Estimation of Li-ion Battery using Unscented Kalman Filter Considering Effects of Temperatures and C-rates. *IEEE Trans. Energy Convers.* **2022**, 1. [CrossRef]
65. Xiong, R.; Cao, J.; Yu, Q.; He, H.; Sun, F. Critical Review on the Battery State of Charge Estimation Methods for Electric Vehicles. *IEEE Access* **2017**, *6*, 1832–1843. [CrossRef]
66. Berecibar, M.; Gandiaga, I.; Villarreal, I.; Omar, N.; Van Mierlo, J.; van den Bossche, P. Critical review of state of health estimation methods of Li-ion batteries for real applications. *Renew. Sustain. Energy Rev.* **2016**, *56*, 572–587. [CrossRef]
67. Wang, Y.; Chen, Z.; Zhang, C. Online remaining energy prediction: A case study in embedded battery management system. *Appl. Energy* **2017**, *194*, 688–695. [CrossRef]
68. Wang, Y.; Zhang, C.; Chen, Z. An adaptive remaining energy prediction approach for lithium-ion batteries in electric vehicles. *J. Power Sources* **2016**, *305*, 80–88. [CrossRef]
69. Feng, F.; Teng, S.; Liu, K.; Xie, J.; Xie, Y.; Liu, B.; Li, K. Co-estimation of lithium-ion battery state of charge and state of temperature based on a hybrid electrochemical-thermal-neural-network model. *J. Power Sources* **2020**, *455*, 227935. [CrossRef]
70. Cabrera-Castillo, E.; Niedermeier, F.; Jossen, A. Calculation of the state of safety (SOS) for lithium ion batteries. *J. Power Sources* **2016**, *324*, 509–520. [CrossRef]
71. Rijanto, E.; Rozaqi, L.; Nugroho, A.; Kanarachos, S. RLS with optimum multiple adaptive forgetting factors for SoC and SoH estimation of Li-Ion battery. In Proceedings of the 2017 5th International Conference on Instrumentation, Control, and Automation (ICA), Yogyakarta, Indonesia, 9–11 August 2017; pp. 73–77. [CrossRef]
72. Zhang, C.; Allafi, W.; Dinh, Q.; Ascencio, P.; Marco, J. Online estimation of battery equivalent circuit model parameters and state of charge using decoupled least squares technique. *Energy* **2018**, *142*, 678–688. [CrossRef]
73. Natella, D.; Onori, S.; Vasca, F. A co-estimation framework for state of charge and parameters of Lithium-ion battery with robustness to aging and usage conditions. *IEEE Trans. Ind. Electron.* **2022**, 1–10. [CrossRef]
74. Ahwiadi, M.; Wang, W. An enhanced particle filter technology for battery system state estimation and RUL prediction. *Measurement* **2022**, *191*, 110817. [CrossRef]
75. Chen, M.; Han, F.; Shi, L.; Feng, Y.; Xue, C.; Gao, W.; Xu, J. Sliding Mode Observer for State-of-Charge Estimation Using Hysteresis-Based Li-Ion Battery Model. *Energies* **2022**, *15*, 2658. [CrossRef]
76. Xue, Z.; Zhang, Y.; Cheng, C.; Ma, G. Remaining useful life prediction of lithium-ion batteries with adaptive unscented kalman filter and optimized support vector regression. *Neurocomputing* **2019**, *376*, 95–102. [CrossRef]
77. Meng, J.; Ricco, M.; Luo, G.; Swierczynski, M.; Stroe, D.-I.; Stroe, A.-I.; Teodorescu, R. An Overview and Comparison of Online Implementable SOC Estimation Methods for Lithium-Ion Battery. *IEEE Trans. Ind. Appl.* **2017**, *54*, 1583–1591. [CrossRef]

78. Xuan, D.-J.; Shi, Z.; Chen, J.; Zhang, C.; Wang, Y.-X. Real-time estimation of state-of-charge in lithium-ion batteries using improved central difference transform method. *J. Clean. Prod.* **2019**, *252*, 119787. [CrossRef]
79. Tian, Y.; Lai, R.; Li, X.; Xiang, L.; Tian, J. A combined method for state-of-charge estimation for lithium-ion batteries using a long short-term memory network and an adaptive cubature Kalman filter. *Appl. Energy* **2020**, *265*, 114789. [CrossRef]
80. Sun, D.; Chen, X.; Ruan, Y. Research on modeling and state of charge estimation for lithium-ion battery. In Proceedings of the 2014 International Power Electronics and Application Conference and Exposition, Shanghai, China, 5–8 November 2014; pp. 1401–1406. [CrossRef]
81. Cui, X.; Jing, Z.; Luo, M.; Guo, Y.; Qiao, H. A New Method for State of Charge Estimation of Lithium-Ion Batteries Using Square Root Cubature Kalman Filter. *Energies* **2018**, *11*, 209. [CrossRef]
82. Qiu, X.; Wu, W.; Wang, S. Remaining useful life prediction of lithium-ion battery based on improved cuckoo search particle filter and a novel state of charge estimation method. *J. Power Sources* **2020**, *450*, 227700. [CrossRef]
83. Linghu, J.; Kang, L.; Liu, M.; Luo, X.; Feng, Y.; Lu, C. Estimation for state-of-charge of lithium-ion battery based on an adaptive high-degree cubature Kalman filter. *Energy* **2019**, *189*, 116204. [CrossRef]
84. Zarei, J.; Kowsari, E.; Razavi-Far, R. Induction Motors Fault Detection Using Square-Root Transformed Cubature Quadrature Kalman Filter. *IEEE Trans. Energy Convers.* **2018**, *34*, 870–877. [CrossRef]
85. Savargaonkar, M.; Chehade, A. An Adaptive Deep Neural Network with Transfer Learning for State-of-Charge Estimations of Battery Cells. In Proceedings of the 2020 IEEE Transportation Electrification Conference & Expo (ITEC), Chicago, IL, USA, 23–26 June 2020; pp. 598–602. [CrossRef]
86. Hong, J.; Wang, Z.; Chen, W.; Wang, L.-Y.; Qu, C. Online joint-prediction of multi-forward-step battery SOC using LSTM neural networks and multiple linear regression for real-world electric vehicles. *J. Energy Storage* **2020**, *30*, 101459. [CrossRef]
87. Lipu, M.S.H.; Hannan, M.A.; Hussain, A.; Saad, M.H.; Ayob, A.; Uddin, M.N. Extreme Learning Machine Model for State-of-Charge Estimation of Lithium-Ion Battery Using Gravitational Search Algorithm. *IEEE Trans. Ind. Appl.* **2019**, *55*, 4225–4234. [CrossRef]
88. Li, I.-H.; Wang, W.-Y.; Su, S.-F.; Lee, Y.-S. A Merged Fuzzy Neural Network and Its Applications in Battery State-of-Charge Estimation. *IEEE Trans. Energy Convers.* **2007**, *22*, 697–708. [CrossRef]
89. Hannan, M.A.; How, D.N.T.; Lipu, M.S.H.; Ker, P.J.; Dong, Z.Y.; Mansur, M.; Blaabjerg, F. SOC Estimation of Li-ion Batteries With Learning Rate-Optimized Deep Fully Convolutional Network. *IEEE Trans. Power Electron.* **2020**, *36*, 7349–7353. [CrossRef]
90. Ni, Z.; Yang, Y. A Combined Data-Model Method for State-of-Charge Estimation of Lithium-Ion Batteries. *IEEE Trans. Instrum. Meas.* **2021**, *71*, 1–11. [CrossRef]
91. Chehade, A.A.; Hussein, A.A. A Multioutput Convolved Gaussian Process for Capacity Forecasting of Li-Ion Battery Cells. *IEEE Trans. Power Electron.* **2021**, *37*, 896–909. [CrossRef]
92. Lipu, M.S.H.; Hannan, M.A.; Hussaion, A.; Ansari, S.S.; Rahman, S.A.; Saad, M.H.; Muttaqi, K. Real-time State of Charge Estimation of Lithium-ion Batteries Using Optimized Random Forest Regression Algorithm. *IEEE Trans. Intell. Veh.* **2022**, 1. [CrossRef]
93. Li, R.; Xu, S.; Li, S.; Zhou, Y.; Zhou, K.; Liu, X.; Yao, J. State of Charge Prediction Algorithm of Lithium-Ion Battery Based on PSO-SVR Cross Validation. *IEEE Access* **2020**, *8*, 10234–10242. [CrossRef]
94. Bian, C.; Yang, S.; Miao, Q. Cross-Domain State-of-Charge Estimation of Li-Ion Batteries Based on Deep Transfer Neural Network with Multiscale Distribution Adaptation. *IEEE Trans. Transp. Electrif.* **2020**, *7*, 1260–1270. [CrossRef]
95. Li, Y.; Wang, C.; Gong, J. A multi-model probability SOC fusion estimation approach using an improved adaptive unscented Kalman filter technique. *Energy* **2017**, *141*, 1402–1415. [CrossRef]
96. Bi, Y.; Choe, S.-Y. An adaptive sigma-point Kalman filter with state equality constraints for online state-of-charge estimation of a Li(NiMnCo)O2/Carbon battery using a reduced-order electrochemical model. *Appl. Energy* **2019**, *258*, 113925. [CrossRef]
97. Sangwan, V.; Kumar, R.; Rathore, A.K. State-of-charge estimation for li-ion battery using extended Kalman filter (EKF) and central difference Kalman filter (CDKF). In Proceedings of the 2017 IEEE Industry Applications Society Annual Meeting, Cincinnati, OH, USA, 1–5 October 2017; pp. 1–6. [CrossRef]
98. Yang, F.; Zhang, S.; Li, W.; Miao, Q. State-of-charge estimation of lithium-ion batteries using LSTM and UKF. *Energy* **2020**, *201*, 117664. [CrossRef]
99. Huang, C.; Wang, Z.; Zhao, Z.; Wang, L.; Lai, C.S.; Wang, D. Robustness Evaluation of Extended and Unscented Kalman Filter for Battery State of Charge Estimation. *IEEE Access* **2018**, *6*, 27617–27628. [CrossRef]
100. Peng, J.; Luo, J.; He, H.; Lu, B. An improved state of charge estimation method based on cubature Kalman filter for lithium-ion batteries. *Appl. Energy* **2019**, *253*, 113520. [CrossRef]
101. Plett, G.L. *Battery Management Systems, Volume II: Equivalent-Circuit Methods*; Artech House: Norwood, MA, USA, 2015; Available online: https://books.google.com/books?id=1kSPCwAAQBAJ&pgis=1 (accessed on 26 September 2022).
102. Shete, S.; Jog, P.; Kumawat, R.K.; Palwalia, D. Battery Management System for SOC Estimation of Lithium-Ion Battery in Electric Vehicle: A Review. In Proceedings of the 2021 6th IEEE International Conference on Recent Advances and Innovations in Engineering (ICRAIE), Kedah, Malaysia, 1–3 December 2021; Volume 6, pp. 1–4. [CrossRef]
103. Fang, L.; Li, J.; Peng, B. Online Estimation and Error Analysis of both SOC and SOH of Lithium-ion Battery based on DEKF Method. *Energy Procedia* **2019**, *158*, 3008–3013. [CrossRef]
104. How, D.N.T.; Hannan, M.A.; Lipu, M.S.H.; Sahari, K.S.M.; Ker, P.J.; Muttaqi, K.M. State-of-Charge Estimation of Li-Ion Battery in Electric Vehicles: A Deep Neural Network Approach. *IEEE Trans. Ind. Appl.* **2020**, *56*, 5565–5574. [CrossRef]

105. Sahinoglu, G.O.; Pajovic, M.; Sahinoglu, Z.; Wang, Y.; Orlik, P.V.; Wada, T. Battery State-of-Charge Estimation Based on Regular/Recurrent Gaussian Process Regression. *IEEE Trans. Ind. Electron.* **2017**, *65*, 4311–4321. [CrossRef]
106. Zhao, R.; Kollmeyer, P.J.; Lorenz, R.D.; Jahns, T.M. A Compact Methodology Via a Recurrent Neural Network for Accurate Equivalent Circuit Type Modeling of Lithium-Ion Batteries. *IEEE Trans. Ind. Appl.* **2018**, *55*, 1922–1931. [CrossRef]
107. Liu, K.; Shang, Y.; Ouyang, Q.; Widanage, W.D. A Data-Driven Approach with Uncertainty Quantification for Predicting Future Capacities and Remaining Useful Life of Lithium-ion Battery. *IEEE Trans. Ind. Electron.* **2020**, *68*, 3170–3180. [CrossRef]
108. Fasahat, M.; Manthouri, M. State of charge estimation of lithium-ion batteries using hybrid autoencoder and Long Short Term Memory neural networks. *J. Power Sources* **2020**, *469*, 228375. [CrossRef]
109. Hu, X.; Che, Y.; Lin, X.; Onori, S. Battery Health Prediction Using Fusion-Based Feature Selection and Machine Learning. *IEEE Trans. Transp. Electrif.* **2020**, *7*, 382–398. [CrossRef]
110. Lyu, Z.; Gao, R.; Chen, L. Li-Ion Battery State of Health Estimation and Remaining Useful Life Prediction Through a Model-Data-Fusion Method. *IEEE Trans. Power Electron.* **2020**, *36*, 6228–6240. [CrossRef]
111. Charkhgard, M.; Farrokhi, M. State-of-Charge Estimation for Lithium-Ion Batteries Using Neural Networks and EKF. *IEEE Trans. Ind. Electron.* **2010**, *57*, 4178–4187. [CrossRef]
112. Hu, X.; Li, S.E.; Yang, Y. Advanced Machine Learning Approach for Lithium-Ion Battery State Estimation in Electric Vehicles. *IEEE Trans. Transp. Electrif.* **2015**, *2*, 140–149. [CrossRef]
113. Chen, J.; Ouyang, Q.; Xu, C.; Su, H. Neural Network-Based State of Charge Observer Design for Lithium-Ion Batteries. *IEEE Trans. Control Syst. Technol.* **2017**, *26*, 313–320. [CrossRef]
114. Li, W.; Sengupta, N.; Dechent, P.; Howey, D.; Annaswamy, A.; Sauer, D.U. Online capacity estimation of lithium-ion batteries with deep long short-term memory networks. *J. Power Sources* **2020**, *482*, 228863. [CrossRef]
115. Bian, C.; He, H.; Yang, S. Stacked bidirectional long short-term memory networks for state-of-charge estimation of lithium-ion batteries. *Energy* **2019**, *191*, 116538. [CrossRef]
116. Chemali, E.; Kollmeyer, P.J.; Preindl, M.; Ahmed, R.; Emadi, A.; Kollmeyer, P. Long Short-Term Memory Networks for Accurate State-of-Charge Estimation of Li-ion Batteries. *IEEE Trans. Ind. Electron.* **2018**, *65*, 6730–6739. [CrossRef]
117. Bian, C.; He, H.; Yang, S.; Huang, T. State-of-charge sequence estimation of lithium-ion battery based on bidirectional long short-term memory encoder-decoder architecture. *J. Power Sources* **2019**, *449*, 227558. [CrossRef]
118. Shu, X.; Li, G.; Zhang, Y.; Shen, S.; Chen, Z.; Liu, Y. Stage of Charge Estimation of Lithium-Ion Battery Packs Based on Improved Cubature Kalman Filter With Long Short-Term Memory Model. *IEEE Trans. Transp. Electrif.* **2020**, *7*, 1271–1284. [CrossRef]
119. She, C.; Wang, Z.; Sun, F.; Liu, P.; Zhang, L. Battery Aging Assessment for Real-World Electric Buses Based on Incremental Capacity Analysis and Radial Basis Function Neural Network. *IEEE Trans. Ind. Informatics* **2019**, *16*, 3345–3354. [CrossRef]
120. Anton, J.C.A.; Nieto, P.J.G.; Viejo, C.B.; Vilan, J.A.V. Support Vector Machines Used to Estimate the Battery State of Charge. *IEEE Trans. Power Electron.* **2013**, *28*, 5919–5926. [CrossRef]
121. Feng, F.; Hu, X.; Liu, J.; Lin, X.; Liu, B. A review of equalization strategies for series battery packs: Variables, objectives, and algorithms. *Renew. Sustain. Energy Rev.* **2019**, *116*, 109464. [CrossRef]
122. Ouyang, Q.; Han, W.; Zou, C.; Xu, G.; Wang, Z. Cell Balancing Control For Lithium-Ion Battery Packs: A Hierarchical Optimal Approach. *IEEE Trans. Ind. Inform.* **2019**, *16*, 5065–5075. [CrossRef]
123. Lee, Y.-S.; Cheng, M.-W. Intelligent Control Battery Equalization for Series Connected Lithium-Ion Battery Strings. *IEEE Trans. Ind. Electron.* **2005**, *52*, 1297–1307. [CrossRef]
124. Song, C.; Shao, Y.; Song, S.; Chang, C.; Zhou, F.; Peng, S.; Xiao, F. Energy Management of Parallel-Connected Cells in Electric Vehicles Based on Fuzzy Logic Control. *Energies* **2017**, *10*, 404. [CrossRef]
125. McCurlie, L.; Preindl, M.; Emadi, A. Fast Model Predictive Control for Redistributive Lithium-Ion Battery Balancing. *IEEE Trans. Ind. Electron.* **2016**, *64*, 1350–1357. [CrossRef]
126. Xue, Q.; Li, G.; Zhang, Y.; Shen, S.; Chen, Z.; Liu, Y. Fault diagnosis and abnormality detection of lithium-ion battery packs based on statistical distribution. *J. Power Sources* **2020**, *482*, 228964. [CrossRef]
127. Schmid, M.; Gebauer, E.; Hanzl, C.; Endisch, C. Active Model-Based Fault Diagnosis in Reconfigurable Battery Systems. *IEEE Trans. Power Electron.* **2020**, *36*, 2584–2597. [CrossRef]
128. Xu, Y.; Ge, X.; Shen, W.; Yang, R. A Soft Short-Circuit Diagnosis Method for Lithium-Ion Battery Packs in Electric Vehicles. *IEEE Trans. Power Electron.* **2022**, *37*, 8572–8581. [CrossRef]
129. Yao, L.; Xiao, Y.; Gong, X.; Hou, J.; Chen, X. A novel intelligent method for fault diagnosis of electric vehicle battery system based on wavelet neural network. *J. Power Sources* **2020**, *453*, 227870. [CrossRef]
130. Shang, Y.; Lu, G.; Kang, Y.; Zhou, Z.; Duan, B.; Zhang, C. A multi-fault diagnosis method based on modified Sample Entropy for lithium-ion battery strings. *J. Power Sources* **2020**, *446*, 227275. [CrossRef]
131. Zhang, X.; Hu, Y.; Deng, J.; Xu, H.; Wen, H. Feature Engineering and Artificial Intelligence-Supported Approaches Used for Electric Powertrain Fault Diagnosis: A Review. *IEEE Access* **2022**, *10*, 29069–29088. [CrossRef]
132. Gao, W.; Zheng, Y.; Ouyang, M.; Li, J.; Lai, X.; Hu, X. Micro-short-circuit diagnosis for series-connected lithium-ion battery packs using mean-difference model. *IEEE Trans. Ind. Electron.* **2019**, *66*, 2132–2142. [CrossRef]
133. Yao, L.; Fang, Z.; Xiao, Y.; Hou, J.; Fu, Z. An Intelligent Fault Diagnosis Method for Lithium Battery Systems Based on Grid Search Support Vector Machine. *Energy* **2021**, *214*, 118866. [CrossRef]

134. Xiong, R.; Yu, Q.; Shen, W.; Lin, C.; Sun, F. A Sensor Fault Diagnosis Method for a Lithium-Ion Battery Pack in Electric Vehicles. *IEEE Trans. Power. Electron.* **2019**, *34*, 9709–9718. [CrossRef]
135. Sidhu, A.; Izadian, A.; Anwar, S. Adaptive nonlinear model-based fault diagnosis of li-ion batteries. *IEEE Trans. Ind. Electron.* **2015**, *62*, 1002–1011. [CrossRef]
136. Zhao, Y.; Liu, P.; Wang, Z.; Zhang, L.; Hong, J. Fault and defect diagnosis of battery for electric vehicles based on big data analysis methods. *Appl. Energy* **2017**, *207*, 354–362. [CrossRef]
137. Lin, T.; Chen, Z.; Zheng, C.; Huang, D.; Zhou, S. Fault diagnosis of lithium-ion battery pack based on hybrid system and dual extended Kalman filter algorithm. *IEEE Trans. Transp. Electrif.* **2020**, 7782. [CrossRef]
138. Li, D.; Zhang, Z.; Liu, P.; Wang, Z.; Zhang, L. Battery Fault Diagnosis for Electric Vehicles Based on Voltage Abnormality by Combining the Long Short-Term Memory Neural Network and the Equivalent Circuit Model. *IEEE Trans. Power Electron.* **2021**, *36*, 1303–1315. [CrossRef]
139. Xia, B.; Shang, Y.; Nguyen, T.; Mi, C. A correlation based fault detection method for short circuits in battery packs. *J. Power Sources* **2017**, *337*, 1–10. [CrossRef]
140. Ojo, O.; Lang, H.; Kim, Y.; Hu, X.; Mu, B.; Lin, X. A Neural Network-Based Method for Thermal Fault Detection in Lithium-Ion Batteries. *IEEE Trans. Ind. Electron.* **2020**, *46*, 1. [CrossRef]